T.C.
ALTINBAS UNIVERSITY
Institute of Graduate Studies
Electrical and Computer Engineering

A NOVEL APPROACH FOR INVESTIGATION OF ELECTROMAGNETIC IMPACT ON HUMAN BODY AND ITS RESPONSE ANALYSIS

Saif AL-SABTI

Doctor of Philosophy

Supervisor
Asst. Prof. Dogu Cagdas Atilla

Istanbul, 2021

A Novel Approach for Investigation of Electromagnetic Impact on Human Body and Its Response Analysis

by

Saif Mohamed Baraa Mohamed Al-Sabti

Department

Electrical and Computer Engineering

Submitted to the Graduate School of Science and Engineering

In partial fulfillment of the requirements for the degree of

Doctor of Philosophy

ALTINBAŞ UNIVERSITY

2021

The thesis titled “A Novel Approach for Investigation of Electromagnetic Impact on Human Body and Its Response Analysis” prepared and presented by “Saif Mohamed Baraa Mohamed AL-SABTI” was accepted as a Doctor of Philosophy Thesis in Electrical and Computer Engineering.

____
Asst. Prof. Dogu Cagdas ATILLA
Supervisor

Thesis Defense Jury Members:

Asst. Prof. Dogu Cagdas ATILLA	Faculty of Engineering and Architecture,	
	Altinbas University	__________________
Prof. Oguz BAYAT	Faculty of Engineering and Architecture,	
	Altinbas University	__________________
Assoc. Prof. Yasa EKSIOGLU OZOK	Faculty of Engineering and Architecture,	
	Altinbas University	__________________
Asst. Prof. Cahit KARAKUS	Faculty of Engineering and Architecture,	
	Esenyurt University	__________________
Asst. Prof. Cagatay AYDIN	Faculty of Engineering,	
	Ege University	__________________

I certify that this thesis satisfies all the requirements as a thesis for the degree of Doctor of Philosophy.

Approval Date of Institute of Graduate Studies:

15/10/2021

I hereby declare that all information in this document has been obtained and presented in accordance with academic rules and ethical conduct. I also declare that, as required by these rules and conduct, I have fully cited and referenced all material and results that are not original to this work.

Saif Mohamed Baraa Mohamed Al-Sabti

Signature

DEDICATION

In the beginning, I thank and thank Allah Almighty for the blessings He has bestowed upon me. I dedicate this work to my dear mother and father, and to my wife and daughters who have endured a lot of patience in achieving the desired goal. I thank everyone who helped me and my supervisor Asst. Prof. Dogu Cagdas ATILLA and friends stood by me. In the end, I thank God for his sincere praise, and prayers and peace be upon the Messenger of God, Muhammad, may God bless him and grant him peace.

ABSTRACT

A Novel Approach for Investigation of Electromagnetic Impact on Human Body And Its Response Analysis

Al-Sabti, Saif Mohamed Baraa Mohamed Al-Sabti

PhD, Department, Altınbaş University,

Supervisor: Asst. Prof. Dogu Cagdas Atilla

Date: October, 2021

Pages: (76)

The thesis discusses three essential topics within the specialization of electromagnetic waves and their impact on humans. The first subject is "The Impact of the Fifth Generation Waves with High Frequencies on the Head and Their Results with a Novel Vision," which contributes the influence of the 5G antenna at high frequency 27.74 GHz on the head's layers to obtain the penetration distance of electromagnetic waves through the layers and state which layer the SAR impact disappear or reduce. Moreover, the role of the head in the reflected radiation pattern, and calculate the sustained energy to benefit from harvesting energy purposes.

The second part is "A Novel Vision for Mathematical Model between Electromagnetic Radiation and Thermodynamic Parameters in Biochemistry Frame "submitted a novel model to find the relation of formulas between the thermodynamics parameters and electromagnetic parameters in biochemistry considerations, The Enthalpy, Internal energy, and Gibbs free energy are perfect indicators for describing bio-reaction in the human body. These formulas control body reactions or *Krebs cycle*. Moreover, the derived formulas convert the reaction from nonspontaneous to spontaneous form by converting Gibbs free energy to a negative value. The increasing electromagnetic waves in the atmosphere due to technological development. Which urges urgently to amend and update all equations to consider the effect of magnetic waves in all disciplines affected them.

The last one is “The Hyperthermia Calculating in Head Blood by the SARs Influence in Novel Vision” The association between SARs and hyperthermia in the human head is discussed in this article using a novel, simple-to-calculate procedure and reliable outcomes. The blood temperature increase is measured using SAR, heat transfer, and the thermodynamic equation. The mass, thickness, thermal conductivity constant, conduction film, volumetric blood flow rate, absorption time, energy absorption region for each layer, and specific heat capacity of the head layers are all regarded. According to these results, the temperature change is determined by actual absorption rate and period of radiation exposure, with head layer properties staying constant. Also, the head layers were found to be capable of withstanding temperature variations.

Keywords: SAR, Electromagnetic field, Head’s blood hyperthermia, Gibbs free energy, Krebs cycle.

TABLE OF CONTENTS

Pages

LIST OF TABLES

Pages

LIST OF FIGURES

Pages

LIST OF ABBREVIATIONS

SAR	:	Specific Absorption Rate
IoT	:	Internet of Things
5G	:	Fifth Generation
ACS	:	Absorption Cross-Section
FCC	:	Federal Communications Commission
OFDM	:	Orthogonal Frequency Division Multiplexing
ATP	:	Adenosine Triphosphate
CST	:	Computer Simulation Technology

LIST OF SYMBOLS

μ	:	Mobility of electron
λ	:	Wave length
ω	:	Angle frequency
U	:	Internal Energy
H	:	Enthalpy
S	:	Entropy
v	:	Velocity
w	:	Weight in Newton (N)
g	:	Gravity acceleration
g_1	:	The Air Gap Between Dipoles
D	:	The electric flux density
B	:	magnetic flux density
J	:	Current density
σ	:	Conductivity
δ_p	:	Skin depth at lossy material
ρ	:	Density
c	:	Specific Heat Capacity
t	:	Time Exposure

F	:	Frequency
G	:	Gibbs Free Energy
PE	:	Potential Energy
KE	:	Kinetic Energy
W	:	Work
U	:	Internal Energy
P	:	Electromagnetic Power Density
z	:	Height
p	:	Pressure
m	:	Mass
A	:	Area
R	:	Resistance
E_{th}	:	Thevenin's Voltage
Ȟ	:	Magnetic Field
j	:	Imaginary
E	:	Energy
Q	:	Heat Transfer
K	:	Dissociation Reaction Equilibrium
Q_k	:	Reaction Quetient

1. INTRODUCTION

Generally, they are many sources of electromagnetic fields in natural and artificially generated by human some of them Cosmic rays, Sun, Antennas, Mobil devices, nuclear fission, high voltage transmission line, Medical device (MRI, CT scan,) and electric vehicle.

As a result of technological development in many aspects of life, the electromagnetic field's use increased in many medical and industrial applications and wireless communication systems. These developed technologies causes raising the concentration of electromagnetic fields in the atmosphere. The electromagnetic fields became effected on all species on the earth directly and non-directly. Moreover, they impact the environment.

The thesis can be classified into three parts. The first part is "The Impact of the Fifth Generation Waves with High Frequencies on the Head and Their Results with a Novel Vision," introduced the influence of the 5G antenna on the head's layers to obtain the penetration distance of electromagnetic waves through the layers. While the second concern A Novel Vision for Mathematical Model between Electromagnetic Radiation and Thermodynamic Parameters in Biochemistry Frame. This paper seeks the relationship between the SARs equations with biological, biochemistry, physical chemistry, and thermodynamics equations. These equations link the outside to the inside of the body to describe the metabolism changes effecting by SAR. The last part is "The Hyperthermia Calculating in Head Blood by the SARs Influence in Novel Vision". This part studies the SAR impact on blood hyperthermia using heat transfer Fourier's law of heat conduction and Newton's law for cooling or convection heat transfer in a novel approach.

The thesis introduces three main subjects.

1.1 THE THESIS INTRODUCES THREE MAIN SUBJECTS

1.1.1 The Impact of the Fifth Generation Waves with High Frequencies on the Head and Their Results with a Novel Vision

The amount of incident radiation absorbed by the body can be presented as the specific absorption rate SAR. It can be expressed in two standard limitation levels for RF signal energy exposure by mobile devices: united states FCC standard is 1.6 watts per kg can be taken over a mass for 1 gram of tissue also its can be estimated over volume and European Union: CENELEC IEC is 2 watts per kg for 10 g of tissue, or it can be expressed for the whole body [1]. It can also express the value of the power density or absorption cross-section ACS [1],[2]. The amount of electromagnetic energy absorbed by the tissue is proportional to the tissue conductivity. It is proportional to the square root of the tissue's dielectric constant. [3], Wearable antennas experience degradation of their performance, like frequency detachment, decrease bandwidth, and distortions of radiation in human body conditions [4]. This study simulated the SAR impact on the Human body head for a 5G antenna device with a frequency of 27.74 GHz to estimate the SAR value at a certain point through the head layers, with many parameters including absorbed power, Maximum point SAR, Minimum point SAR and others. CST (computer simulation technology) had been used for simulation.

1.1.2 A Novel Vision for Mathematical Model between Electromagnetic Radiation and Thermodynamic Parameters in Biochemistry Frame

The goal of this research is to develop a mathematical model that can be used to build a connection between biochemistry processes in the body, which are focused on physical chemistry, and the efficacy of the RF electromagnetic field's absorbed energy, which SAR represents.

This method develops a novel model that may be used for sensing, metabolic regulation, degradation, decomposition, and the creation of biological processes in all bodily tissues.

The mathematical model for electromagnetic energy absorbed by tissues is derivable using the following crucial variables: exposure intensity, frequency, source distance from the body, exposure area concentration, polarization, and incidence angle. The most vital of these factors are energy exposure. This parameter is significant because it represents the quantity of energy transmitted into the human body and the frequency of electromagnetic waves determining the depth of signal energy entering human tissues [1].

The purpose of this research is to combine two fields: the impact of physical chemistry caused by biological processes in the body and the effect of regulated electromagnetic radiation on the human body. To reconcile the two ideas, we developed a novel method. First, in terms of electromagnetic fields, the energy released by the source is partly absorbed by the body. It denotes the rate of specific energy absorption (SAR) [1]. Second, in terms of physical chemistry, a rise in the energy produced by the body as a result of external energy absorption or living activities is another component, denoted by the symbol U for internal energy change.

Physical chemistry is a useful subject for acting bioprocess relationships since it can be used to determine if biological processes are endothermic or exothermic. Physical chemistry quantifies the amount of energy contained in various components such as lipids, proteins, saccharides, and starches, as well as the amount of energy that can be released from these components. Apart from dissolving into basic elements such as carbon dioxide and water, these biological molecules may be broken into smaller units such as (protein to an amino acid, lipid to lipoamide). Almost all reactions in the human body are endothermic. Finally, all bonds in any materials or components must get sufficient energy to be broken. Numerous variables may be considered: Gibbs free energy, Internal energy, enthalpy, temperature, and entropy [5, 6, 7, 8].

1.1.3 The Hyperthermia Calculating in Head Blood by the SARs Influence in Novel Vision

Many researchers study the absorption of electromagnetic waves to the human, animal, or plant bodies by calculating the specific absorption rate or the absorbed electromagnetic field's energy [9, 10, 11]. Studies dealt with electromagnetic waves on the body or head in terms of heat or electromagnetic waves' interaction on the metabolism process [10, 11, 12]. Some of them deal with reducing the effect of electromagnetic waves' specific absorption rate to reduce their effects [13]. This research focuses on with the study of several values of the specific absorption rate (SAR) and its effect in terms of thermal change in the blood of the head with different periods, taking into consideration the constant of thermal conductivity related to each layer and film conductance of blood's layer as well as the area of each layer.

1.2 CONTRIBUTIONS

1.2.1 The Impact of the Fifth Generation Waves with High Frequencies on the Head and Their Results with a Novel Vision

The study contributes the influence of the 5G antenna at high frequency 27.74 GHz on the head's layers to obtain the penetration distance of electromagnetic waves through the layers and state which layer the SAR impact disappear or reduce besides show how much energy absorbed, sustain, reflected and incident. Moreover, what is the role of the head in the reflected radiation pattern, and how to calculate the sustained energy to benefit from harvesting energy purposes? Furthermore, specifying the head layer may infect by cancer in the future.

1.2.2 A Novel Vision for Mathematical Model between Electromagnetic Radiation and Thermodynamic Parameters in Biochemistry Frame

This research combine multi-field to gathers in a novel approach. It show the relationship among electromagnetic equation, the SAR, thermodynamic, biochemistry, physical chemistry. Furthermore, it states the ability to control the bio-reaction and the metabolism in human body. This article show the SAR effect to the state function parameters (ΔH, ΔG, ΔS). They are very good indication for the body's reaction. Especially Gibbs free energy to convert from nonspontaneous reaction to spontaneous reaction. . These mathematical models will simulate and interpret many of the results of experimental research conducted without mathematical expression. This study will add terms to the equations in many disciplines with consideration of the electromagnetic field effect.

1.2.3 The Hyperthermia Calculating in Head Blood by the SARs Influence in Novel Vision.

This study contributes to using a new and more efficient method to introduce heat transfer Fourier's law of heat conduction and Newton's law for cooling or convection heat transfer and thermodynamic equations with SAR equations electromagnetic power [1, 14, 15]. The presented method is considered one of the easiest computational methods with actual results dependent on the head layers' nature physics and biological properties. This paper concerns the SARs effectiveness on the white matter layer and the blood and how heat is transferred through the artery. Besides, it appears the potential resistance for each layer against the electromagnetic power absorbed. Furthermore, it is submitted easy method to present the SAR limitation in the working environment. This study will open new vistas in this type of research.

2. LITERATURE REVIEW

a. The shield reduces electromagnetic waves. By inserted the shield inside or outside the cell phone, the exact output yield with the mobile antenna and the SAR reduction as well as could place it in the cell phone back of the cover case for practical use [13].

b. As the frequency increases, we have a more outstanding SAR and heat effect, exceeding skin limits set by ICNIRP, the European Commission, and IEEE-ICES. Besides, high power release 3.6 kW, 7.2 kW, 11 kW) technology is also being offered on electric cars. In a few years, portable gadgets will undoubtedly be anywhere in the house, at work, and in public space, and we will increasingly face electromagnetic fields. We will also improve our potential research to analyze this wireless development in human health and electricity [16].

c. The present study makes swift measurements of different thermal signatures following EM and RF treatments. As such, the values of such a particular absorption rate (SAR) for biological tissues may be measured at various intervals, offering an insight into the impact on biological tissues of electromagnetic waves exposure. The present work also offers a computational solution for measuring dielectric and other relevant properties for different tissue changes following thermal treatments. This analysis would also improve researchers' awareness and experience of post-therapy tissues' actions while helping to efficiently and quickly modify procedures for therapeutic therapies [11].

d. The production and improvement of radiofrequency hyperthermia therapies are essential when exposed to electromagnetic waves. These minimally invasive therapies may be a safer option than surgery and radiation therapy [17].

e. Hyperthermia induced by nanoparticles for cancer care is an increasing field of cancer Nano medicine since the capacity for localized and selective cancer cell death. The treatment depends on several variables, including bio-Nano fluid thermal conductivity, Nano particular volume, wavelength, power arousal, and metabolic heat [18].

f. We anticipate the established voxel models used in several fields of study and examine the electromagnetic field. We intend to render accessible to the public data from the built models for usage. Different studies, adopting the conditions of specific delivery [19].

g. The usage of body energy harvesters for power supply is a recent sector that needs more exploration and development creating a feasible technology. Body energy-driven wearable appliances will reduce the global battery environmental effect and save millions of dollars in electricity costs annually [20].

h. Hyperthermia of the most well-known effect of SAR is Microwave hyperthermia uses temperatures to treat cancer effectively. An antenna system fitted with a cooling device (a water shot) can be applied to avoid radiation side effects. Optimizing the specific absorption rate (SAR) in the tumor means maximizing it, or into directly high-temperature regions. A way to accomplish low-complexity planning with temperature it’s caused by the thermal boundary layer and by-body mechanics such as airflow in the respiratory tracts which cause SAR shifts. Focusing on the tumor using SAR assists with temperature does it while accounting for the impacts of the antenna excitations comparing temperatures to obtain a SAR point that maximizes the chosen objective. The method's consistent application to the 3D head and neck region delivers superior temperature coverage regardless of the uncertainties in thermal parameters. This improvement is reached by solving the bio-heat equation a few times, removing it from the global optimization [18].

i. This novel infrared temperature-based wireless exposure approach was reported in this study. The findings of this research indicate that IRT is applicable for body surface temperature tracking, employing the sensor. Additionally, this research shows that IR temperature-based RF safety assessment may be used to generic RF devices of various frequencies and power levels 30-minute computations of the SAR followed, based on temperature and model bio-heat were performed. Orientation of simulated and real tissue motions was substantial and critical. The SAR was 32 microwatts per kilogram, for simulations and 35 grams per kilogram and for reconstruction after that this made the SAR readings almost in compliance with the world regulations of 2 kilogram the highest temperature never rose over one degree Celsius. An IRT value of about 8.7% different from the SAR values shown in the tables the measurement sensitivity is 108 Karth & Rama Rao wouldn't go below 32 mW/kg. Accuracy and sensitivity in IR thermometry will be enabled by the methodology. Evaluation of the SAR at high frequency requires greater heating depths, since the frequencies are lower to find out whether the SAR calculated using the suggested might produce varying upper and lower limits for temperature rise and power levels [12].

3. METHODOLOGY

3.1 METHODOLOGY OF A NOVEL VISION FOR THE IMPACT OF THE FIFTH GENERATION WAVES WITH HIGH FREQUENCIES ON THE HEAD AND THEIR RESULTS WITH A NOVEL VISION

Methodology summarizes into several points:

a. The Dipole Antenna has been designed at 5G on Ka-band at a center frequency 27.74GHz, as the electromagnetic field's source on the distance from the head 2.7 mm where the dipole is proposed.

b. Taking voxel model (phantoms) head then exposure electromagnetics wave at a high frequency according to 5G mobile networking. We have constructed the head layers by using CST simulation software. To obtain the effectiveness of the microwave signals on the head, for finding the power absorption (SAR) and reflecting. Furthermore, finding the distance of penetrating the microwave signals through the head layers.

c. Study radiation pattern and its direction by changing the antenna positions respected to the head.

d. Calculate the SAR, the sustained power on the head skin due to incident power, and the reflected power.

e. According to above how to guess the location of hazardous pathogens in part of the head layers depending on some factors?

3.1.1 Antenna Design

The Dipole Antenna has been designed at 5G on Ka-band at a center frequency 27.74GHz, as the electromagnetic field's source on the distance from the head 2.7 mm where the dipole is proposed.

The center frequency 27.74GHz for 5G mobile networking has been selected depending on Federal Communications Commission FCC 15-138 [21].

The equations design of the dipole is:

For $L=\lambda/2$ and $\lambda/2 < L < \lambda$, L is the dipole's length [22].

The equation of the dipole design is [23]:

$$L = \frac{143}{f_{\circ}} \tag{3.1}$$

$$g_1 = \frac{L}{200} \tag{3.2}$$

g_1 is the air gap between dipoles.

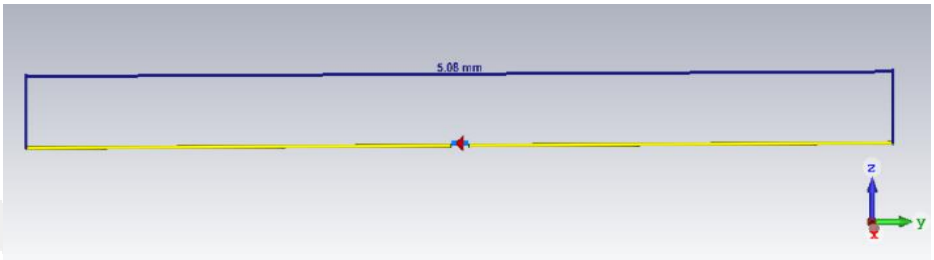

Figure 3.1 (a): The antenna measurements

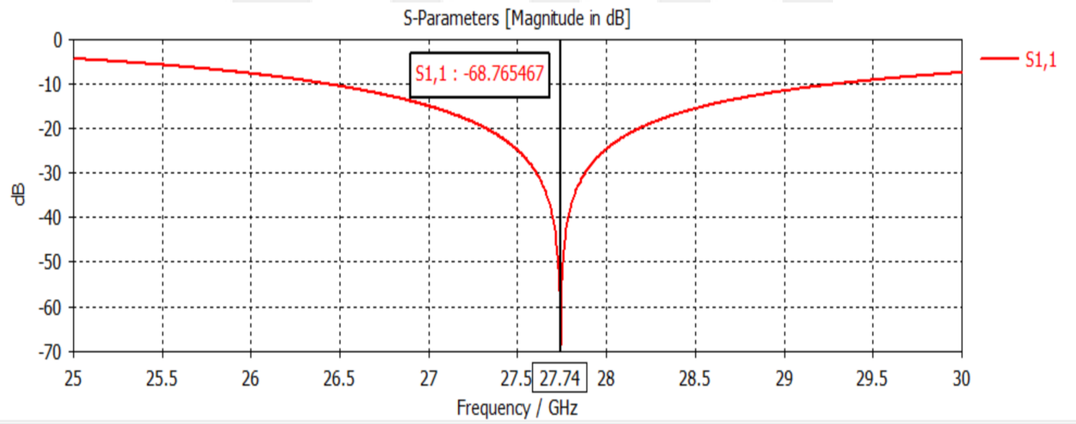

Figure 3.1 (b): The return loss S_{11} curve

Figure 3.1(b) S_{11} curve of the dipole antenna works at a center frequency of 27.74 at -70 dB. It has been designed by computer simulation technology CST studio suite. The Antenna bandwidth is 2.6GHz.

3.1.2 SAR Equations Calculation

The SAR (specific absorption rate) has a biological effect on body tissue that causes an increase in the body tissues' internal energy or causes some physical change in tissue or a specific point that power absorption occurs like temperature rising, metabolism increasing. The SAR depends on frequency values, type of tissues, the sum of power incident to the body, the distance between the source and the body, material permittivity, angle of power incident, the geometry of the body, and quantity of power source. There are two standard SAR limitations FCC and IEC, as was previously explained in the introduction, so this study is dependent on IEC standards [1].

The parameters and equations that describe the amount of SAR are presented [1].

$$J = Jo\ e^{\frac{-x}{\delta_p}} \tag{3.3}$$

$$J = \sigma E \tag{3.4}$$

$$\delta_p = \frac{1}{\omega \sqrt{\frac{\mu_0\ \varepsilon_0\ \varepsilon'}{2}[\sqrt{1 + (\frac{\varepsilon''}{\varepsilon'})^2} - 1]}} \tag{3.5}$$

$$SAR = \frac{\sigma\ [E]^2}{2\rho} \tag{3.6}$$

$$SAR = c\frac{\triangle T}{\triangle t} \cong 4186 c_H \frac{\triangle T}{\triangle t} \tag{3.7}$$

J is Current density, σ is Conductivity, δ_p Skin depth at lossy material, ρ is Density, c is specific heat capacity for human tissues in J/Kg K, and $\triangle t$ is a time exposure.

The equation. (7) Describes the hyperthermia on the skin surface and the peripheral layers in which the SAR is reached.

3.1.3 Methodology Implementation and Results

This proposed study simulated SAR impact through the human head for 5G high frequency. The dipole antenna is independently designed and generates a voxel head segment to import the dipole antenna where the voxel model head is accessible. Both of them set the same boundary and set the parameters expected to produce productive results, as seen below:

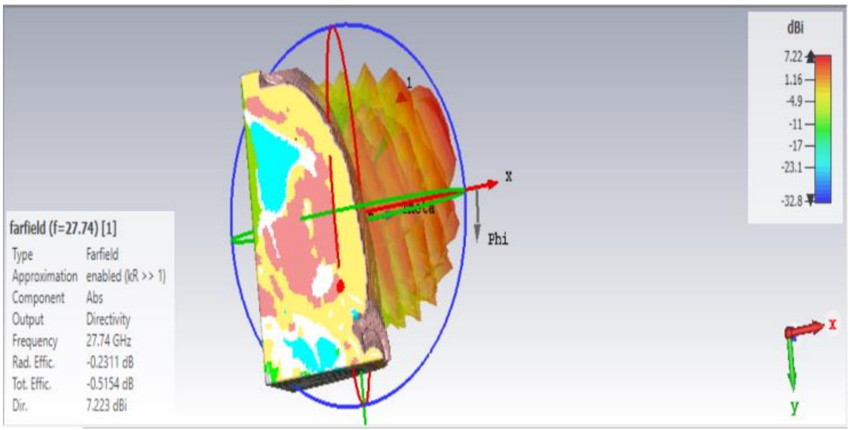

Figure 3.2 (a): The radiation pattern directivity (7.22 dB) at point (35, -40, 45) of the Dipole antenna.

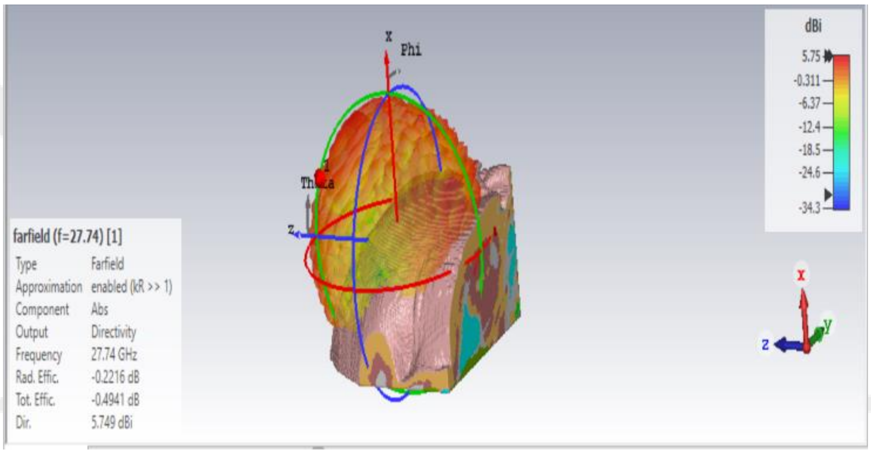

Figure 3.2 (b.1): The radiation pattern directivity (5.75 dB) at point (35, 0, 45) of the dipole antenna.

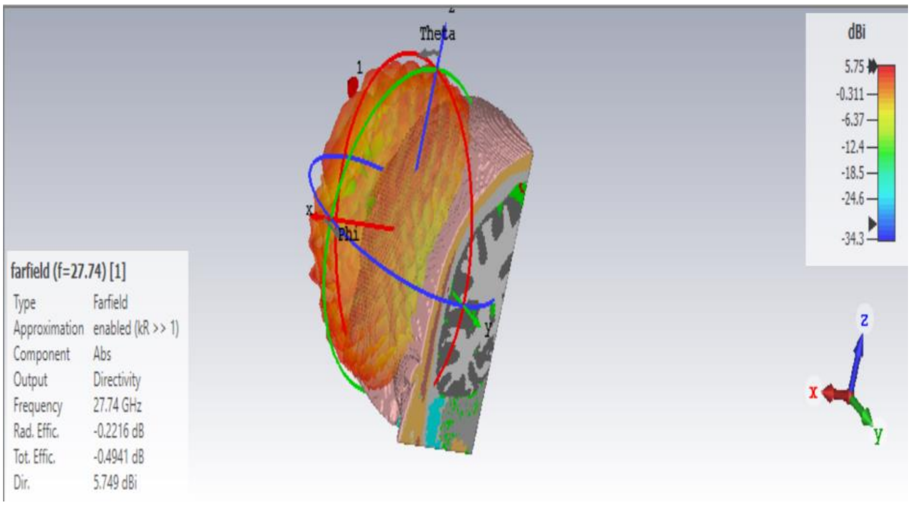

Figure 3.2 (b.2): The radiation pattern directivity (5.75 dB) at point (35, 0, 45) of the dipole antenna.

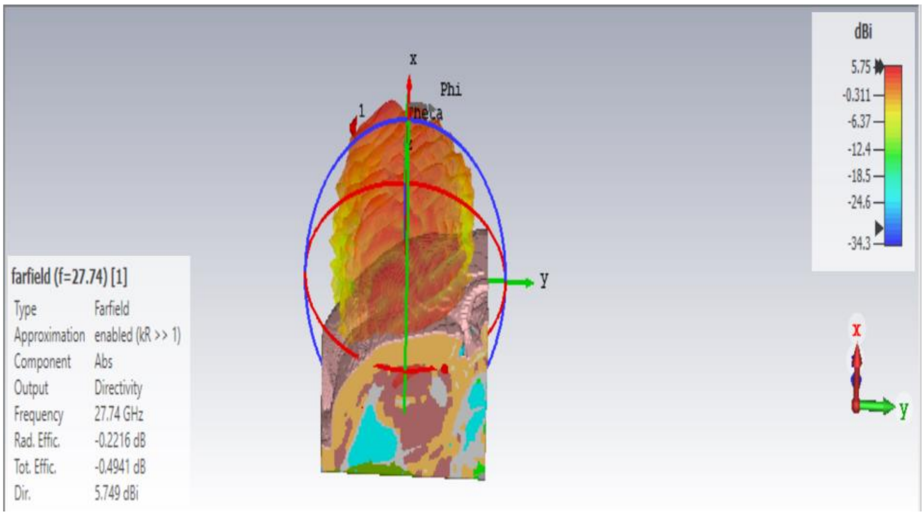

Figure 3.2 (b.3): The radiation pattern directivity (5.75 dB) at point (35, 0, 45) of the dipole antenna.

Fig. 3.2 (a) And (b) represent the human head of the voxel model work as a parasitic element reflector for the dipole. Therefore, the figure states the final radiation pattern from their combination effects. The radiation pattern directivity is changed about 180^0 by head effectiveness where the head radiation side is part. Also, as the shape shows, there is no radiation inside the brain or head. The changing values of directivity are due to the transition in dipole location and the angle radiation at two different points. The shapes (b) illustrate the radiation pattern configuration according to head shape.

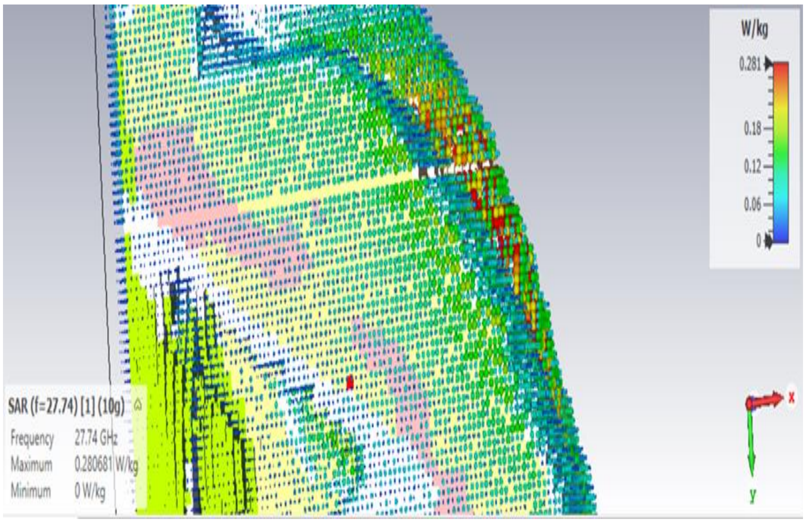

Figure 3.3 (a.1, Vitro): Inside of the Head layers below the skin (Vivo). On and through the skin surface and bit of bone tissue layers of the Head (Vitro) at SAR 0.281 at reference antenna point (35, -40, 45).

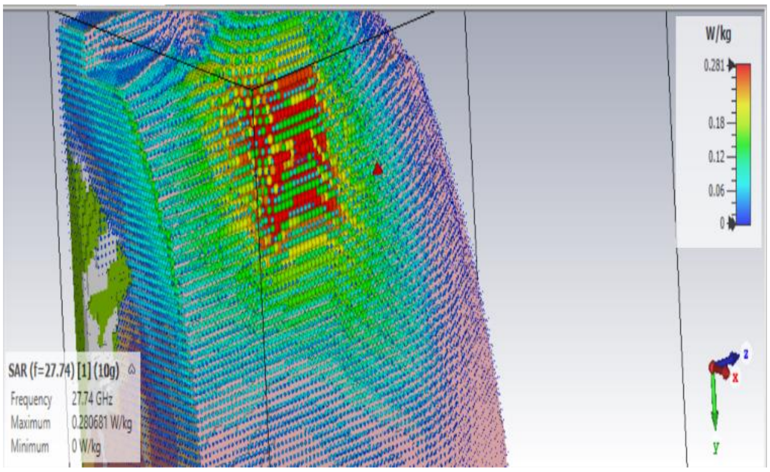

Figure 3.3 (a.2, Vivo): Inside of the Head layers below the skin (Vivo). On and through the skin surface and bit of bone tissue layers of the Head (Vitro) at SAR 0.281 at reference antenna point (35, -40, 45).

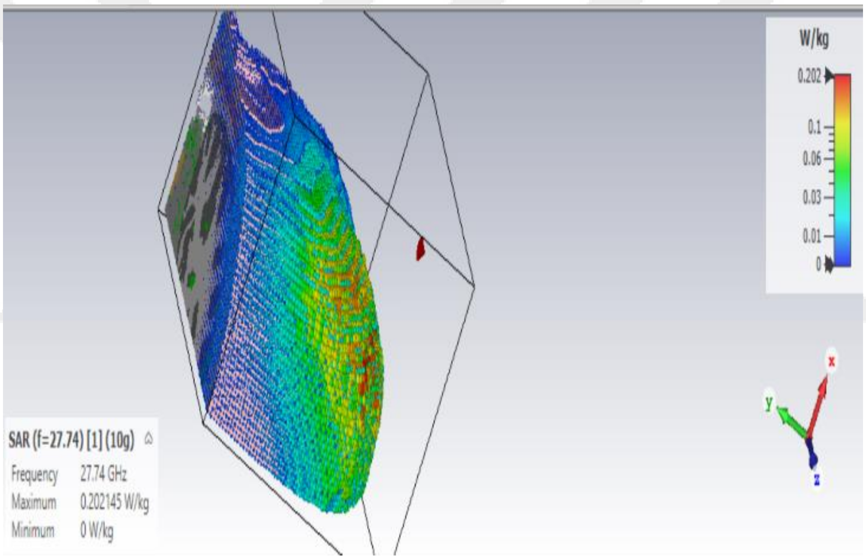

Figure 3.3 (b.1, Vitro): Inside of the Head layers below the skin (Vivo). (Over and Through) the skin surface and a few part bone tissue layers of the Head (Vitro) at SAR 0.202 at reference antenna point (35, 0, 45).

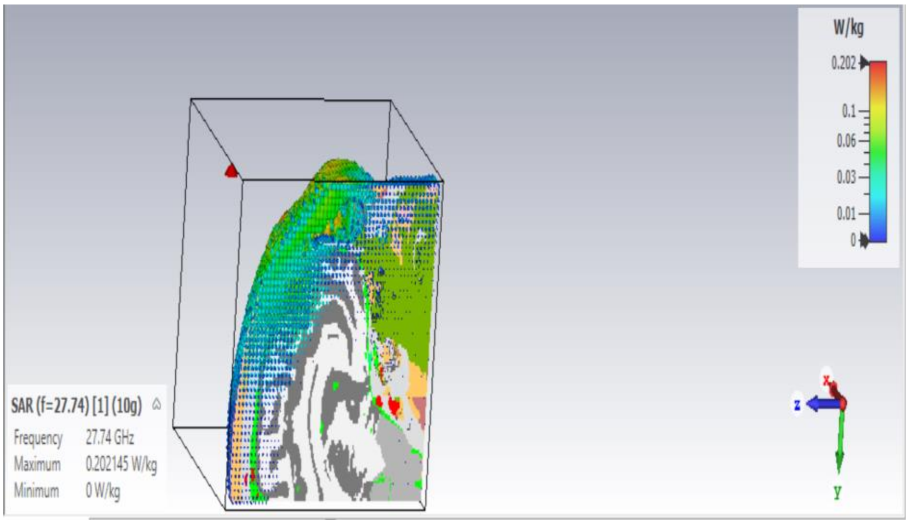

Figure 3.3 (b.2, Vitro): Inside of the Head layers below the skin (Vivo). (Over and Through) the skin surface and a few part bone tissue layers of the Head (Vitro) at SAR 0.202 at reference antenna point (35, 0, 45).

In all part of Fig. 3.3 is represented by the SAR distribution value absorbed through the head from minimum and maximum values. The shape (a) expresses the value of SAR 0.281 at point (35, -40, 45) and (b) the SAR estimation is 0.202 at point (35, 0, 45). Different value of the SAR yields to change the position of the dipole antenna. Both (a) And (b) represent the SAR impact Vitro and Vivo cases in the head. In the vitro case, the most power absorbed occurs from an incident power source, whereas, in vivo, there is no power absorbed.

In general, the most amount of the power incident is reflected in the vitro layer. Then the others give the SAR value. Firstly, there are several reasons: Firstly, RF signal at 5G frequency of 27.74 GHz, the permittivity and conductivity of head skin tissues are related to skin depth. Secondly, head geometry causing effects on reflection. Moreover, the angle of the RF signal incident and the amount of power source.

3.2 METHODOLOGY OF A NOVEL VISION FOR THE MATHEMATICAL MODEL BETWEEN ELECTROMAGNETIC RADIATION AND THERMODYNAMIC PARAMETERS IN BIOCHEMISTRY FRAME

3.2.1 Mathematical Expression

Generally, there are three types of the systems:-

a. An open system is permitted to alter its mass and heat transfer coefficients in response to its surroundings. The open system may be divided into the following categories:

   i. Steady-state: The quantities entering the system, such as mass and heat, or a combination of the two, are equal to the amounts exiting. It remains constant throughout time.

Input-output=0 or input=output

   ii. Unsteady-state: The mass or heat, or both, entering the system is not equivalent to the mass or heat leaving it. They fluctuate throughout time in this instance, either increasing or decreasing input.

b. In a closed system, there is no change in mass but just a change in temperature.

c. Isolated system; in a non-flow system, there is no change of mass or heat.

According to thermodynamics' first law, the energy (mass and heat) balance may be represented as follows. [5, 7]:

$$In = Out + Accumulation \tag{3.8}$$

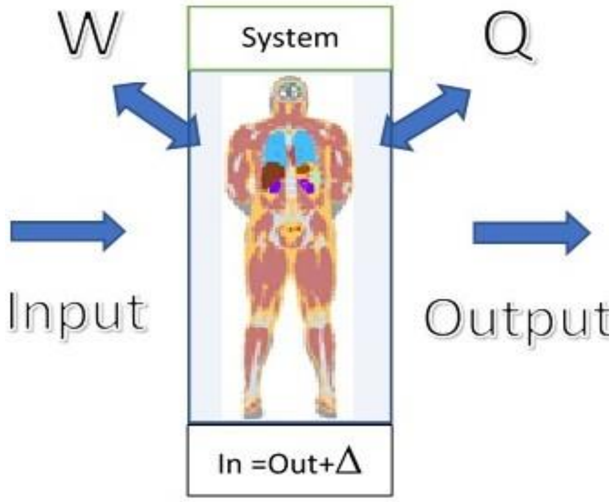

Figure 3.4: Consideration of the human body as a system: The energy and mass balance on the human body.

The Potential Energy in watt is

$$PE = w \times z = m \times g \times z \tag{3.9}$$

w= Weight in Newton (N), m: Mass, g: Gravity acceleration, z: Height

The Kinetic Energy in (watt) is

$$KE = m\frac{v_i^2}{2} \tag{3.10}$$

v: velocity.

U: Internal energy

And the work can be express

$$W_k = p \times V \tag{3.11}$$

W_k: work, p: pressure, V: volume.

∂m_i is mass flowrate input to the system

∂m_o is mass flowrate output to the system

∂Q is the quantity of heat transfer to the system

∂w_k is the quantity of the work done by the system

As the energy balance in the equation (3.8)

Now, if mass ∂m_i is input to the system, the energy of the system increases by

$$Input = \partial mi\, [u_i + p_i V_i + v_i^2 / 2 + gz_i]$$

And the mass ∂m_o output from the system, the energy of the system decreases by an amount

$$Output = \partial mo\, [u_o + p_o V_o + v_o^2 / 2 + gz_o]$$

The total energy change of the system

$$Accumulate = \partial m\, [u + v^2 / 2 + gz]$$

Generally, the total energy within the system boundary may change either because:

a. Change in the mass of the system.
b. Change in the state of the fluid within the system.

Substitute in (3.8) to obtain:-

$$\partial Q + \partial m\, [u_i + p_i V_i + \frac{v_i^2}{2} + gz_i] = \partial w + \partial m\, [u_o + p_o V_o + \frac{v_0^2}{2} + gz_o] + \partial m\, [u + \frac{v^2}{2} + gz] \quad (3.12)$$

Enthalpy varies according to both the internal energy and works their change.

$$H = U + PV \quad (3.13)$$

Where H is Enthalpy

Substitute (3.13) in (3.12)

$$\partial Q + \partial m \left[H_i + \frac{v_i^2}{2} + gz_i\right] = \partial w + \partial m \left[H_o + \frac{v_0^2}{2} + gz_o\right] + \partial m \left[u + \frac{v^2}{2} + gz\right] \quad (3.14)$$

Through the human body, Potential energy and Kinetic energy are neglect.

The equation (3.13) becomes:

$$\partial Q + \partial m\,[H_i] = \partial w + \partial m\,[H_o] + \partial mu \tag{3.15}$$

Rearrange (3.15) to get the general formula of the first law of thermodynamic, which can express as the open system and close system:

$$\partial Q + \partial m\,[H_i] = \partial w + \partial m\,[H_o] + \partial mu \tag{3.16}$$

$$\partial mu + \partial m\,[H_o] - \partial m\,[H_i] = \partial Q - \partial w \tag{3.17}$$

So the mass balance is

$$m_o - m_i = m \tag{3.18}$$

For a close system, the changing of mass equal zero

These are properties of a close system.

$$\partial m_o = 0\,, \partial m_i = 0 \tag{3.19}$$

Therefore, the heat balance is:

$$\partial u + \partial\,[H_o] - \partial\,[H_i] = \partial Q - \partial w_k \tag{3.20}$$

Take the integral for (3.20).

$$\int \partial u + \int \partial\,[H_o] - \int \partial\,[H_i] = \int \partial Q - \int \partial w_k \tag{3.21}$$

$$\Delta U = Q - W_k \tag{3.22}$$

The equation (3.22) is the first low for a close system in thermodynamic.

Whereas the work

$$W_k = \Delta\,(PV) \tag{3.23}$$

So there is no work done on the system (The human body).

Finally, the human body can be described as a close system to give the relation below:

$$\Delta U = Q \tag{3.24}$$

Where $\Delta U \ and \ Q$ In joule

According to the equations of the electromagnetic field [2], drive start from Maxwell's equations

$$\nabla \times E = -\frac{\partial B}{\partial t} \tag{3.25}$$

$$\nabla \times H = J + \frac{\partial D}{\partial t} \tag{3.26}$$

$$\nabla . D = \rho \tag{3.27}$$

$$\nabla \cdot B = 0 \tag{3.28}$$

Where

D is the electric flux density (coul/m^2), B is magnetic flux density (wb/m^2), ρ is electric charge volumetric density, and J is the surface density of electric current.

They are the electric and magnetic fields connected to the electric charges and Currents in the interactive relationship. The so-called constitutive relations complement Maxwell equations.

$$D = \varepsilon E \tag{3.29}$$

$$B = \mu H \tag{3.30}$$

ε is electric permittivity (F/m).

μ is the magnetic permeability (H/m).

E is electric field (V/m).

H is magnetic field (A/m).

The electrical permittivity defines the macroscopic interaction of the electric vector and the dielectric substance, while the magnetic permeability describes the interaction of the material with the magnetic field.

Rewriting the equations (3.25) through (3.26) in the frequency domain by taking Fourier transfer. Moreover, consideration (3.29 and 3.30) use in (3.27 and 3.28).

$$\nabla \times E = -j\omega\mu H \tag{3.31}$$

$$\nabla \times H = \sigma E + j\omega\varepsilon E \tag{3.32}$$

$$\nabla . (\varepsilon E) = \rho \tag{3.33}$$

$$\nabla \cdot (\mu H) = 0 \tag{3.34}$$

ω is The angular frequency.

Using curl operator on (3.31) and (3.32)

To find a vector wave equation for electric field formulation from (3.31).

$$\nabla \times (\nabla \times E) = j\omega\mu\nabla \times \mathrm{H} = -j\omega\mu(J + j\omega\varepsilon E) \tag{3.35}$$

$$\nabla \times (\nabla \times E) - \omega^2\mu\varepsilon E = -j\omega\mu J \tag{3.36}$$

To obtain a vector wave equation with its magnetic field formulation from (3.32).

$$\nabla \times (\nabla \times H) - \omega^2\mu\varepsilon H = \nabla \times \frac{J}{\varepsilon} \tag{3.37}$$

The trivial anisotropy in human tissues and materials simplifies the total anisotropy. The electrical permittivity shape of the tensor into a scalar and complex magnitude.

$$\varepsilon = \varepsilon_o \left(\varepsilon' - j\varepsilon''\right) \tag{3.38}$$

$$\varepsilon r = \frac{\varepsilon}{\varepsilon_o} = \varepsilon' - j\varepsilon'' = \varepsilon'(1 - j \tan \delta) \tag{3.39}$$

ε': The dielectric constant.

ε'': The loss factor.

ε_r: The relative electric permittivity.

δ: The dielectric loss tangent.

The dielectric constant usually communicates the potential of the Electrical energy storage material and the loss factor (or the loss tangent) defines the dissipation of energy attributable to dielectric polarization mechanisms [24].

To understand dielectric dissipation and the conduction or ohmic losses, it is also essential to expand the importance of the electric permittivity, as the distinction is not generally feasible by applying the rule of Ohm.

$$J = \sigma E \tag{3.39}$$

In homogeneous form in (3.36)

$$\nabla \times (\nabla \times E) - \omega^2 \mu \left(\varepsilon - j\frac{\sigma}{\varepsilon}\right) E = 0 \tag{3.40}$$

To compare with (3.36), effective electric permittivity is:

$$\varepsilon_{eff.} = \varepsilon - j\frac{\sigma}{\omega} \tag{3.39}$$

The conduction does not change the dielectric constant. The loss factor can be modified.

$$\varepsilon_{eff.} = \varepsilon_o \left(\varepsilon' - j\varepsilon'' - j\frac{\sigma}{\omega \varepsilon_o}\right) = \varepsilon_o \left(\varepsilon_{eff.}.' - j\, \varepsilon_{eff.}''\right) \tag{3.40}$$

$$\varepsilon_{eff.}.' = \varepsilon' \tag{3.41}$$

The ionic conductance the effect is inversely proportional for the frequency operating

$$\varepsilon_{eff.}'' = \varepsilon'' + j\frac{\sigma}{\omega\varepsilon_o} \tag{3.42}$$

The loss tangent can be described:

$$Tan\ \delta eff = \frac{\varepsilon_{eff.}''}{\varepsilon_{eff.}.'} \tag{3.43}$$

The effective conductivity which responsible for dielectric losses in comparison to the real loss factor,

$$\varepsilon eff'' = \frac{\sigma_{eff}}{\omega\varepsilon_o} \rightharpoonup \sigma_{eff} = \omega\varepsilon_o\varepsilon_{eff.}'' = \omega\varepsilon_o\varepsilon_{eff.}.'\ tan\ \delta eff \tag{3.44}$$

The skin influence is a fascinating phenomenon linked to conductivity. It is typically connected to electrical conductors and can be defined as a high-frequency electric field tending to disperse in a conductor such that the current density near the surface is substantially greater than that of its nucleus with an exponential decline.

$$J = J_O\ e^{-\frac{X}{\delta_\rho}} \tag{3.45}$$

J_o is current density surface

δ_p is penetration depth.

For electric conductivity can be found.

$$\delta_p = \frac{1}{\sqrt{\pi f \mu \sigma}} \tag{3.46}$$

For lossy dielectric material

$$\delta_p = \frac{1}{\omega\sqrt{\frac{\mu_0\ \varepsilon_0\ \varepsilon'}{2}[\sqrt{1+(\frac{\varepsilon''}{\varepsilon'})^2}-1]}} \tag{3.47}$$

Necessary to consider that tan δ < 1 for biological tissues indicates that the dielectric constant ε calculates the wave's penetration into the body. Once radiofrequency energy (i.e., the absorbed power per volume unit) is the distribution of the electric field in the tissue, the heat produced per volume unit and time unit [W / m3] can be represented as from, as below [2],

$$Qgen\ (x,y,z)\ =\ \pi f \varepsilon_o\ \varepsilon''(x,y,z)\ [E(x,y,z)] \tag{3.48}$$

$$Qgen\ (x,y,z)\ =\ \frac{1}{2}\sigma(x,y,z)[E(\ x,y,z\ )]^2 \tag{3.49}$$

The integration can obtain the total power absorption in human tissue throughout all tissues of the human.

$$P =\ \pi f \varepsilon_o \int_V \varepsilon''(\ x,y,z\ ) = [E(\ x,y,z\ )]^2\ dV \tag{3.50}$$

What is SAR (Specific Absorption Rate)?

SAR is the amount of power absorbed by the body tissues per unit mass. It refers to the amount of electromagnetic power has absorbed by human tissues or any object [2].

$$SAR = \frac{1}{V}\int \frac{\sigma(r)[E(\ r)]^2}{\rho(r)} dr \tag{3.51}$$

$$SAR = \frac{\sigma\ [E]^2}{\rho} \tag{3.52}$$

Whereas $J\ =\ \sigma\ E$ induce current density in human biological tissues where J denoted in A/m^2

Therefore:

$$SAR = \frac{J^2}{\rho\sigma} \tag{3.53}$$

The temperature tissues rise in the human body due to induce current density. This increase is proportional to the increase in SAR linearly. In this case, no thermoregulation process (including body metabolism), no heat transfer consideration, and the Heating loss is not occurred. The SAR can be expressed according to these conditions as below:

$$SAR = c\frac{\triangle T}{\triangle t} \cong 4186 c_H \frac{\triangle T}{\triangle t} \tag{3.54}$$

c is specific heat capacity for human tissues in (J/Kg K)

c_H is specific heat capacity in (Kcal/Kg.K)

The relation between internal energy and SAR.

This research demonstrates the internal energy correlated with certain essential variables in body tissue, including;

a. The body's metabolism,
b. The biochemical reaction is affected.
c. Enthalpy-related.
d. The potential energy for chemical reactions has been limited to maximize reactive material efficiency.

Furthermore, these variables are consistent with the SAR influence. As a result of equations (3.24).

Whereas $\Delta U = Q = m\ c\ \Delta T$ in joule

$$E_{Energy} = \Delta U \tag{3.55}$$

$$Power = \frac{Energy}{time} \tag{3.56}$$

Whereas power is in watt

Therefore:

$$P \times \Delta t = \Delta U = Q = m\, c\, \Delta T \tag{3.57}$$

Divided both sides of the equation (3.57) by m and Δt to obtain:

$$SAR = \frac{P}{m} = c\frac{\Delta T}{\Delta t} \tag{3.58}$$

Use the equations (3.52, 3.53, 3.54, 3.57, and 3.58) to get:

$$SAR = \frac{\Delta U}{m\Delta t} = \frac{Q}{m\Delta t} = \frac{J^2}{\rho\sigma} \tag{3.59}$$

$$SAR = \frac{\Delta U}{m\Delta t} = \frac{Q}{m\Delta t} = \frac{J^2}{\rho\sigma} = \frac{P}{m} = c\frac{\Delta T}{\Delta t} = \frac{\sigma\,[E]^2}{\rho} \tag{3.60}$$

In equation (6)

H=U+Δ (PV) if there is no change in pressure and volume.

$$\Delta H = \Delta U = Q \tag{3.61}$$

The equation (3.61) is proved from equations (3.13) and (3.22).

Enthalpy is a measure of the behavior of chemical or biological reactions. The human body is in equilibrium. As a result, every step-change induced inside the body results in a change in a biochemical process. As a result, we can determine the amount of energy released, acquired, or expressed as an endothermal, exothermal, or biological response.

Thus, this study increases our knowledge and understanding of the SAR effect on the body and how to use it to control chemical reactions under directed power while avoiding the harm associated with excessive power (uncontrolled power), as well as which frequency is optimal for obtaining the desired enthalpy and Gibbs free energy for a particular reaction such as fat burning. Boosting the recovery of injured tissues, particularly after surgery Apart from the computation, all variables are conjugated for the reactant components.

Hence the equation becomes:

$$SAR = \frac{\Delta H}{m\Delta t} = \frac{Q}{m\Delta t} = \frac{J^2}{\rho\sigma} = \frac{P}{m} = c\,\frac{\Delta T}{\Delta t} = \frac{\sigma\,[E]^2}{\rho} \tag{3.62}$$

This study could be composed in another way to express the SAR in Thevenin's and Norton's theorems.

$$SAR = \frac{E_{th}^2}{mR_{th}} = R_N * I^2{}_N \tag{3.63}$$

The above model can be used to express for equivalent circuit design integrated with/into the body.

3.2.2 SAR effect on material reactions in body tissues. In consideration of SAR effects in body tissues, Hess's Law has a crucial role [8]:

According to Hess's principle, changes in Enthalpy throughout a chemical reaction (i.e., the reaction heat under constant pressure) are independent of the direction of the reaction from the first to the final phases.

In other words, if a chemical transition occurs through several distinct routes, the resulting enthalpy change is same.

In mathematical terms [5, 7]:

$$\Delta H_{Reactions} = \sum H_{f(Reactants)} - \sum H_{f(Products)} \tag{3.64}$$

ΔH_f is an enthalpy formation.

The enthalpy value raises with the SAR effect as shown below:

$$\Delta H_{new.} = \Delta H_{old} + \Delta H_{SAR} \tag{3.65}$$

Therefore, the overall Enthalpy in the human tissues is expressed in all reactions or bio-reaction occur in the body.

The enthalpy parameter is critical in describing the status of the body's responses as a consequence of the impacts. Hess's law is also applicable to entropy ΔS and Gibbs free energy ΔG.

The body's chemical reactions have occurred when the reactant has enough activation energy E_{Act}, which has the difference between minimum energy E_{min} and reactants energy E_{Rec} to convert into the product as in figure 3.5(a). The figure illustrates the reactants have a different level of energy before a reaction occurs. Three aspects of the reactants' behavior are as follows:

a. Reactants have a low energy level.

b. The reactants lack sufficient activation energy to transform into the product.

c. All reactants have a minimal activation energy for converting substances to products.

The products are always more stable than the reactant because their energy is less than the reactants. The liberation energy (Releasing energy) E_{Rel} is the difference between reactants energy E_{Rec} and product energy E_{Prod}.

$$E_{Act} = E_{min} - E_{Rec} \tag{3.66}$$

$$E_{Rel.} = E_{Rec} - E_{Prod} \tag{3.67}$$

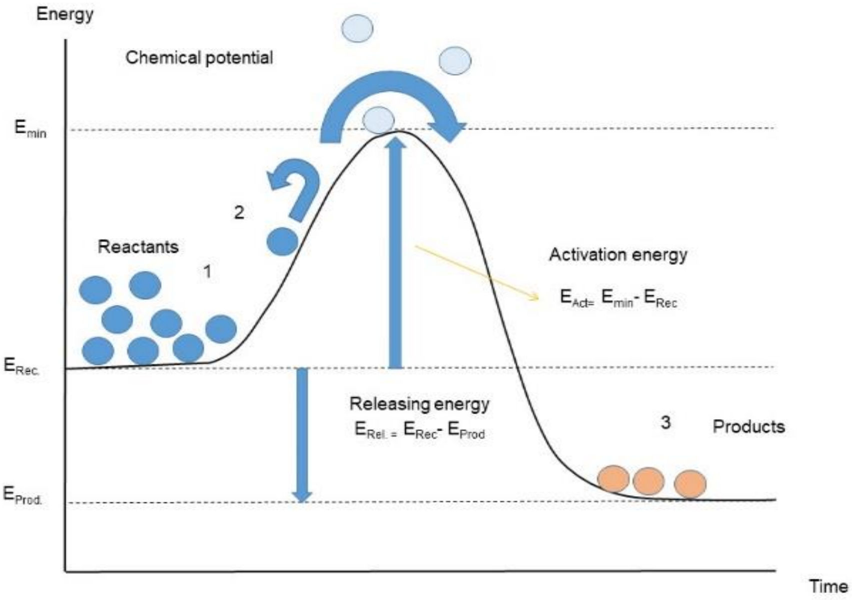

(a)

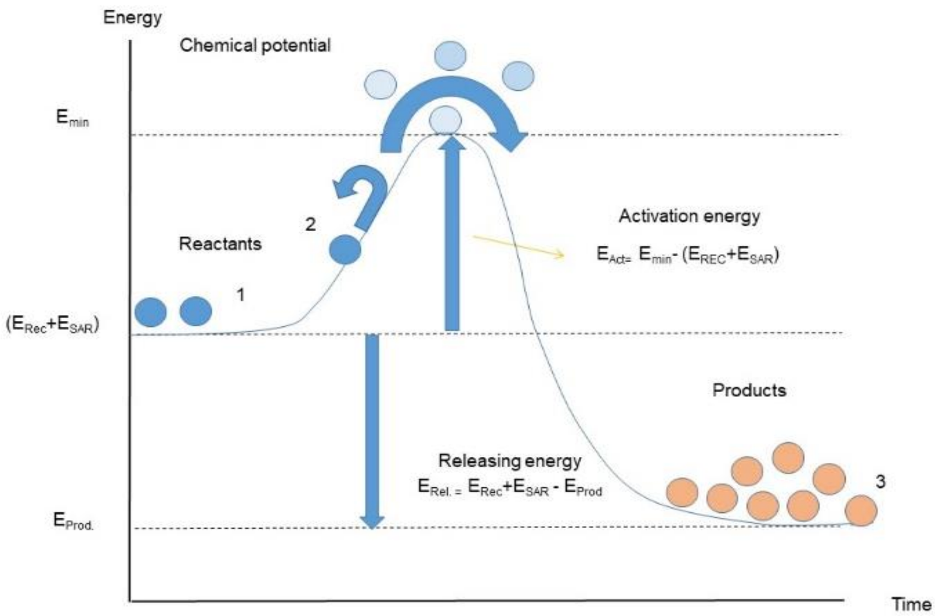

(b)

Figure 3.5: The energy effectiveness on the reactions in the body

(a) Without the SAR consideration

(b) With the SAR consideration

When the human tissues absorb the electromagnetic energy, the whole body gains new energy levels that involve the body's original energy and SAR energy ($E_{SAR.}$). In this case, the almost reactants substances are reacted due to the barrier of activation energy E_{Act} is decreased. For this reason, the amount of product is increased as noted in part 3 in Fig. 3.5 in (b)

$$E_{Act} = E_{min} - (E_{Rec} + E_{SAR}) \tag{3.68}$$

On the other hand, in Fig. 3.5 The energy emitted for chemical reactions by the effectiveness of SAR in (b) is higher than (a), which depends on the amount of SAR as shows below:

$$E_{Rel}. = E_{Rec} + E_{SAR} - E_{Prod} \tag{3.69}$$

3.2.3 Gibbs Free Energy ΔG and Entropy ΔS are affected by The SAR

Entropy ΔS is a measure of randomness and disorder in a system. The greater the randomness or disturbance, the greater the entropy [5, 7].

$$\Delta S_{univ} = \Delta S_{surr} + \Delta S_{sys} \tag{3.70}$$

The SAR increases the randomness.

$$\Delta S_{new} = \Delta S_{old} + \Delta S_{SAR} \tag{3.71}$$

The Gibbs free energy is a thermodynamic potential for measuring the highest reversible work that a thermodynamic system will do at a constant temperature and pressure. It is a state variable that expresses whether a chemical reaction is spontaneous or nonspontaneous. If negative value.

The reaction will be spontaneous. If $\Delta G = 0$ the reaction at the equilibrium otherwise $\Delta G > 0$ positive value, the response becomes nonspontaneous [7, 25].

The Gibbs free energy does not depend on the path that reaction takes place, but it depends on the final state and initial state [5, 7].

Gibbs free energy change equals total energy change for system subtracts energy lost in disordering the system [5, 7].

$$\Delta G^{o}_{sys} = \Delta H^{o}_{sys} - T\Delta S^{o}_{sys} \quad (3.72)$$

$$\Delta G^{o}_{R} = -RT \ln K \quad (3.73)$$

K is the dissociation reaction equilibrium

$$\Delta G^{o}_{Rec} = \sum \Delta G_f^{o}\,(products) - \sum \Delta G_f^{o}\,(reactants) \quad (3.74)$$

Where Q_k = reaction quotient

When $Q_k < K$ or $Q_k > K$, the reaction is spontaneous

At non-standard conditions, ΔG is a change in free energy. ΔG is related to ΔG°

$$\Delta G = \Delta G^{\circ} + RT \ln Q_k \quad (3.75)$$

When ΔG = 0 then $Q_k = K$ reaction is at equilibrium. ΔG is significant to control the reactions that occur in the human body [5, 7]. The SAR is affected by ΔG as it converts the reaction from nonspontaneous to spontaneous and verse versa. The SAR increased the non-order in the system causes rising entropy and increasing the Enthalpy as exothermic ΔH<0 negative also, the SAR causes the shifting at the equilibrium region at ΔG=0 more substance reactant to react to give more products which are shifted in the right direction toward product to increase productivity.

The measurement unit of ΔG is the joule.

$$SAR = \frac{\Delta G}{m\Delta t} \quad (3.76)$$

This equation is considered a more comprehensive expression of control over the interactions that occur throughout the body. The spontaneous domain’s increase by SAR effects due to the equilibrium shifting point at ΔG=0 to the right.

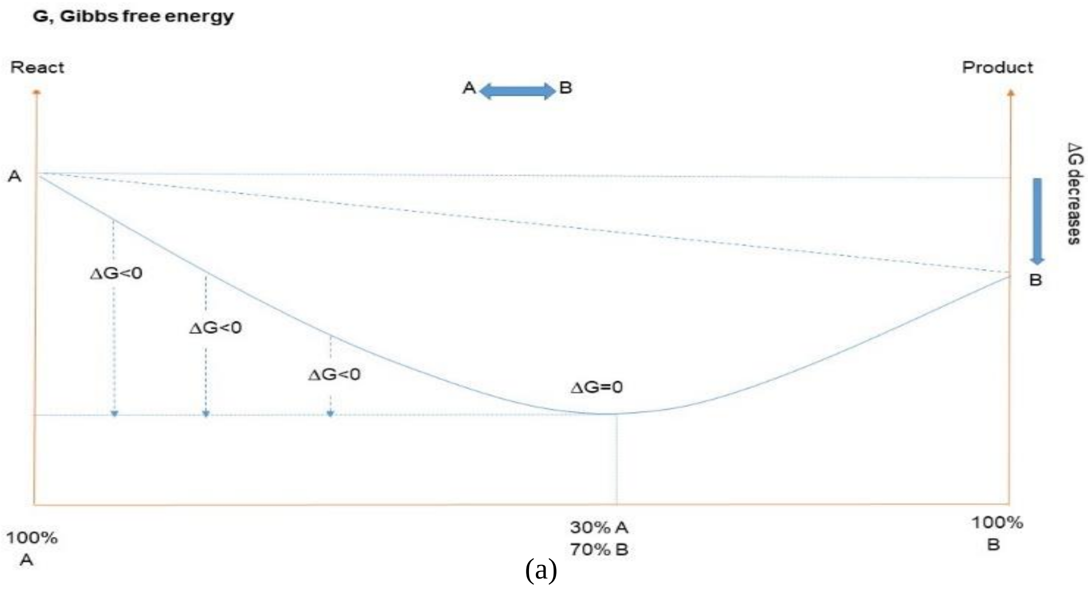

(a)

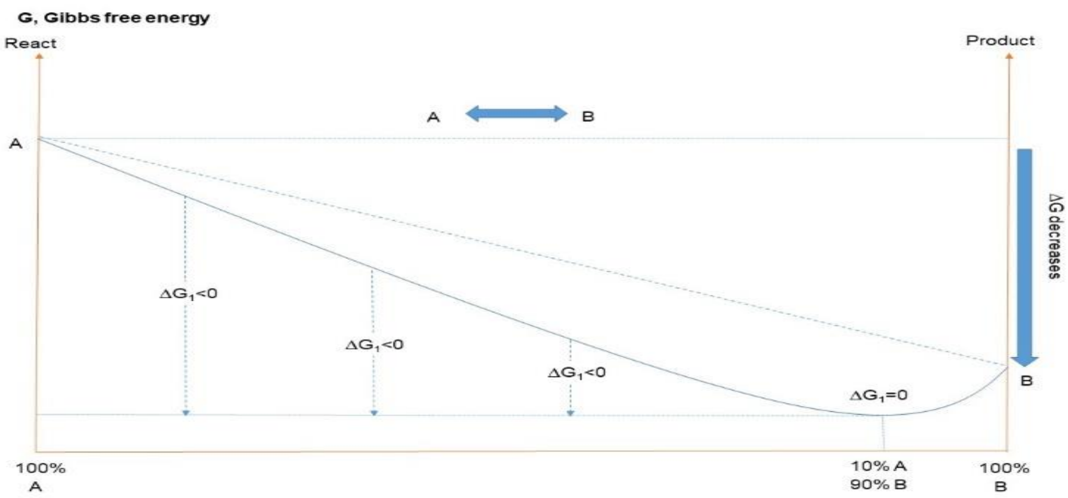

(b)

Figure 3.6: The relation between Gibbs free energy ΔG and constant equilibrium reaction K.

a) Without SAR effects.

b) SAR effects.

Equilibrium Mix near to product K< 1

The figure 3.6 (a) ΔG is negative, and K>1 leads to the reaction go to the right (product > reactant) without SAR effects [25].

The figure 3.6 (b) Equilibrium Mix near to product K< 1 G_{SAR} increases G's negative value to give the final state of ΔG1, and K>1 leads to the reaction more shitted to the right to yield more product close the completion and reactant increase consumption by SAR affects.

Both Fig. 3.5 and Fig. 3.6 Is interpreted what is happened in the results of both references [26] and [27].

3.2.4 Case Study

ATP hydrolysis reaction is one of the most significant reactions in the human body. In glycolysis and Glycogenesis cycles, ATP (adenosine triphosphate) plays a significant part in the metabolism process. Chemiosmosis is the main reason for ATP synthesis [25, 28].

This process transfers protons prepared by Krebs cycle through select channels through the mitochondria membrane (energy houses) from the inside to the outside. The hydrogen proton diffuses through the transporter protein [6, 8, 28].

Every ATP molecule will release 7.3 kilocalories of mole energy.

$$ATP \rightleftarrows ADP + PI$$

$$\Delta G = \Delta G^{\circ} + RT\, ln\, Q_k \tag{3.77}$$

The equilibrium constant as following below [4, 8]

$$Keq = \frac{[products]}{[Reactants]} \tag{3.78}$$

$$Keq = \frac{[ADT][PI]}{[ATP]} \tag{3.79}$$

For non-equilibrium chemical reaction. Q has used the equation (3.75) become [24]:

$$\Delta G = \Delta G^{\circ} + RT\, ln \frac{[ADT][PI]}{[ATP]} \tag{3.80}$$

Where ΔG°_{ATP} = -30.5 KJ at standard condition (25^0 C and 1 atm.) [8].

The human body's temperature is 37^0C. Therefore the gap between the two ΔG is computed below [7, 8]:

$$\Delta G^0_{ATP}(T_2) = \left(1 - \frac{T_2}{T_1}\right)\Delta H^0 + \frac{T_2}{T_1}\Delta G^0_i(T_1) \tag{3.81}$$

SAR has taken placed through the body tissue the overall value of ΔG has been increasing for the whole inside body can be presented:

$$\Delta G_{new} \ = \Delta G_{\ old} + \Delta G_{SAR} \tag{3.82}$$

ΔG_{old}: the entire body without SAR effect.

ΔG_{SAR}: Generating by SAR.

$\Delta G_{\ new}$: Total value with SAR effect.

Reflecting the SAR impact on the equation. (3.78)

$$\Delta G\ new \ = \ \Delta G^{\circ} \ + \ RT\ ln\frac{[ADT][PI]}{[ATP]} \tag{3.83}$$

Since the ΔG° is constant and gain new value of ΔG_{new}. The second term of the above equation increase and, then generate more component concentration decomposition of $[ADT][PI]$ and release more energy.

The other SAR consequence is a rise in the tissue temperature that often contributes to an increase in free energy (3.81) by (3.82):

$$\Delta G^{\circ}_{ATP\ new}(T_2) = \left(1 - \frac{T_2}{T_1}\right)\Delta H^{\circ} + \frac{T_2}{T_1}\Delta G^{\circ}_i(T_1) \tag{3.84}$$

As described above with SAR, thermodynamic equations increase the metabolism by increasing the energy of a whole body's reaction.

SAR's consequence on the other variables is that ΔG's importance is increased indirectly, such as hydrogen [H] [6, 8].

Concluding, SAR values have an exponential influence on the biochemical reaction within the body.

Many practical experimental studies in this orientation that do not have a mathematics model, such as [26, 27], can be described using the above equations model.

3.3 METHODOLOGY OF THE HYPERTHERMIA CALCULATING IN HEAD BLOOD BY THE SARS INFLUENCE IN NOVEL VISION

3.3.1 Blood Distribution in the Human Body and Main Arteries That Have Head Supplying of Blood from the Heart

The heart is the most important organs.it pumps the blood to each part of the body across vascular circulation system. The head connects with upper vascular system. The proportion of blood in the head is 15% of the blood pump by the heart [14].

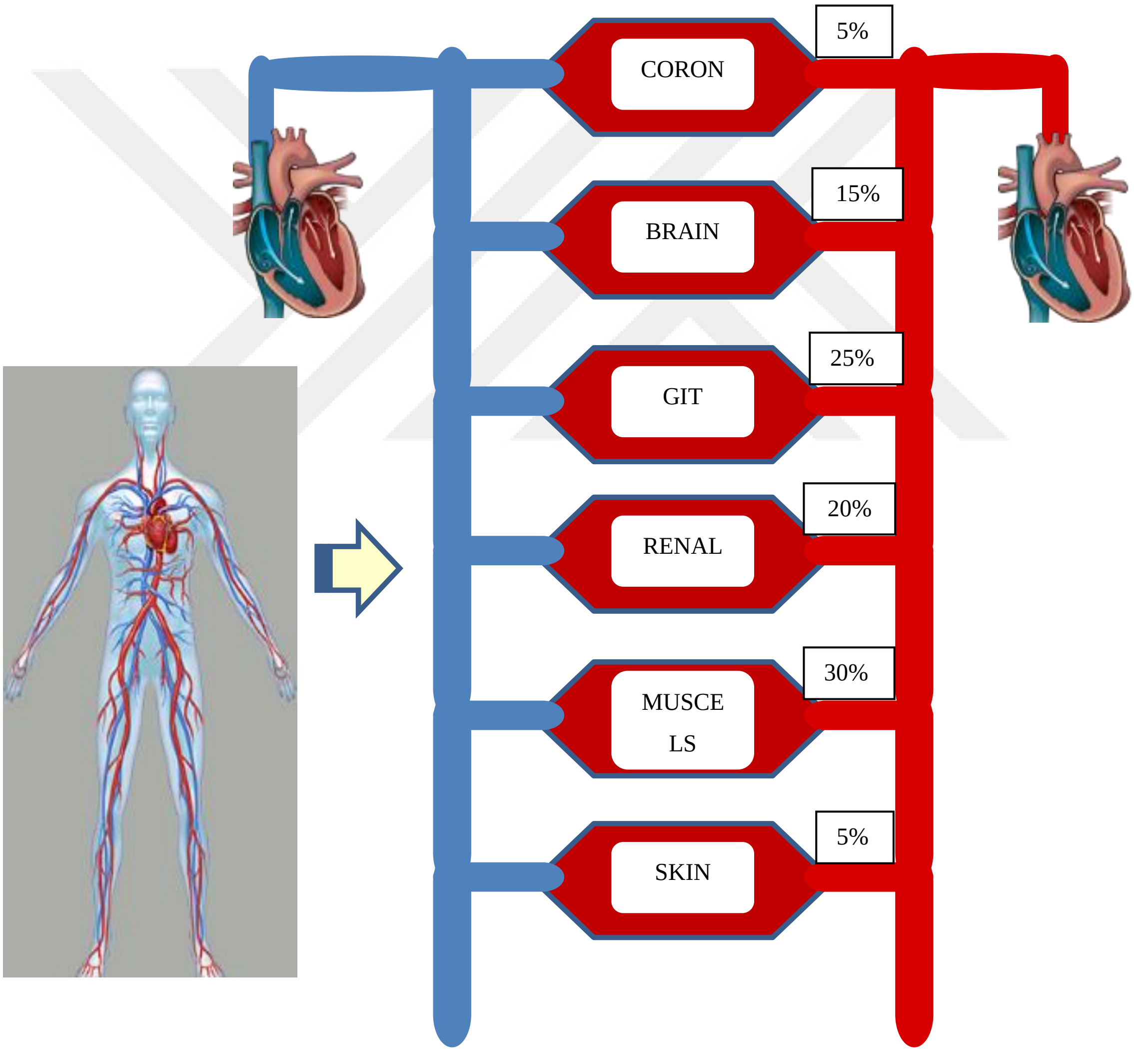

Figure 3.7: The Blood percentages distribution of vascular circulation of the human body parts.

The main arteries symmetrical on the two sides of the head that supply blood to the head are two internal carotids, two external carotids and, two vertebral. The two vertebral combines into one artery to form the basilar artery. The arteries' mean diameter have to be obtained from the below table [29-34]:-

Table 3.1: Arteries diameters

The diameter (mm) of the artery		
Artery name	Minimum	Maximum
Internal Carotid Artery	2.81	4.2
Basilar Artery	1.9	4.15
External Carotid Artery	3	6

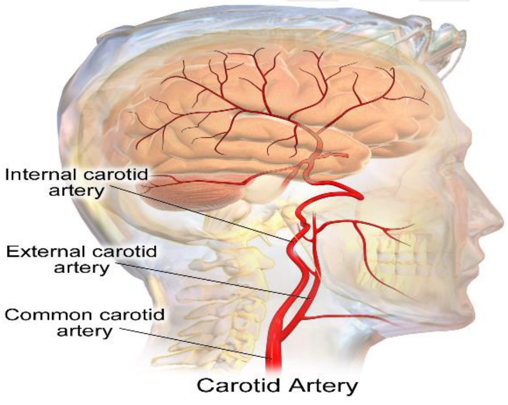

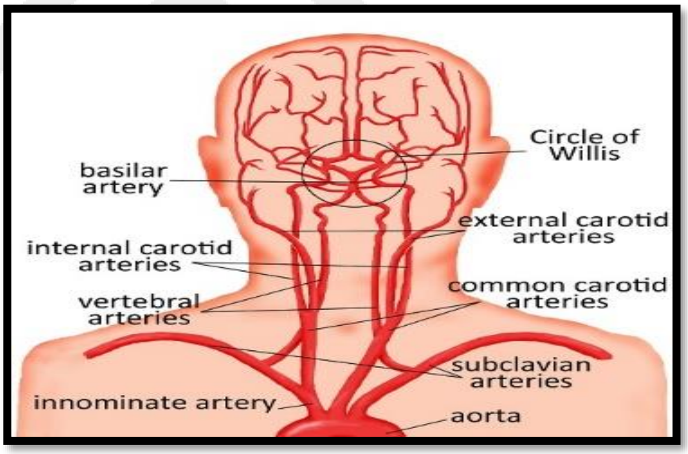

Figure 3.8: The names of the most important arteries that supply blood to the head and show the upper vascular circulation [35]

The presented study is based on the values of arterial diameters and their numbers that are used in the heat transfer calculations as shown in the table below:

Table 3.2: The arteries diameters with their summation

Arterial diameters supply blood to the head in mm		Number
Basilar Artery	3.025	1
Internal Carotid Artery	3.505	2
External Carotid Artery	3.4	2
Total Diameter	16.835	

These arteries' diameters' values change according to age, diseases, weight, gender. Etc.

3.3.2 Requirements, Which are considered in The Calculation of Hyperthermia in The Blood

The most crucial information for an estimate of the SAR impact on blood hyperthermia inside the head layers the physical, thermal properties, or thermodynamics characteristics of head layers [36]. Furthermore, the thickness of the heads' layers. As well as the values of the SAR or Electromagnetic power density absorbed, and the direction of RF waves, the mass of each head's layer, the flowrate of the blood into the artery. The parameters depended are summarized in tables:-

Table 3.3: Head's thickness and thermal characteristics of the layer

Head layers Parameters [35-36]				
Layers	Thickness in mm	$c \frac{J}{°C \cdot Kg}$	$k \frac{W}{m \cdot °C}$	$\rho \frac{Kg}{m^3}$
Skin	2.5	3500	0.42	1010
Fat	3	2500	0.25	920
Skull	6.5	1300	0.4	1810
Cerebrospinal Fluid (CSF)	3.2	4000	0.6	1010
Gray Matter	38	3700	0.57	1040
White Matter	25.1	3600	0.5	1040
Blood	--	3900	0.51	1060

The solutions' strategies represent the head's layers of the human body as an electric circuit. The solution depends on the supper position theorem to estimate the total current and the voltage across specific resistance [38, 39]. There are two sources of the circuit with multi-resistance in series. The head's layers stand as resistances. Moreover, the temperature difference between the layers acts as the EMF electromotive force or potential generating the current in the circuit. Eventually, the heat transfer is expressed as the electrical current.

The first source is the temperature difference inside the artery until it reaches the skin surface. Another source is temperature on the skin's surface is generated from the SAR (specific absorption rate) and the artery core temperature.

(a)

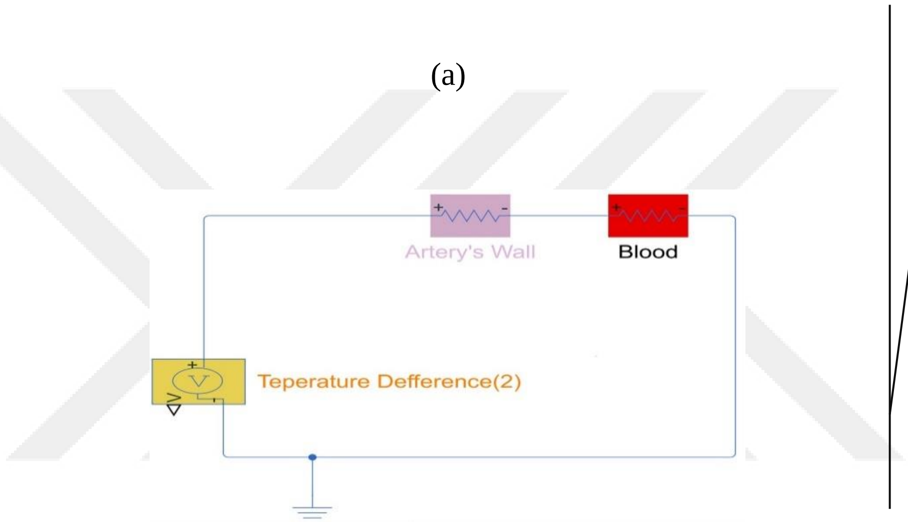

(b)

Figure 3.9: The equivalent circuit of heat transfer calculation

(a) The main system

(b) The subsystem

3.3.3 Procedures of the Heat Transfer and Assumptions:

The heat transfer of the head layers calculation can be done into several parts for obtaining more clarification:

a. Determining the heat transfer from white Matter to the skin's surface to estimate the heat liberated from the skin.
b. Finding the heat's net generated from the SAR equal 1.6 absorbed by the skin across through the head layers to white matter end and the heat generated from the blood that penetrates the head layers releases from the skin.

c. Finding the heat output from the inside of the artery that contains blood to the white Matter surface when the layer begins.

d. Obtaining the result of heat transfer that penetrates the artery's wall till the blood in the arteries' center, by subtracting the heat entered of the Artery and Blood from the heat release of them.

In order to start the procedure some assumption must be considered such as:

A closed system allows the exchange of heat, but a mass exchange has not occurred. Besides this, the system is steady, and the heat transfer happens in one direction. So there is no heat radiation in the system because the calculation begins at the skin's surface. The same region begins to absorb RF power on the head's layers arranged in series as in the figure below. The system is considered a closed system and has heat conduction besides heat convection in blood.

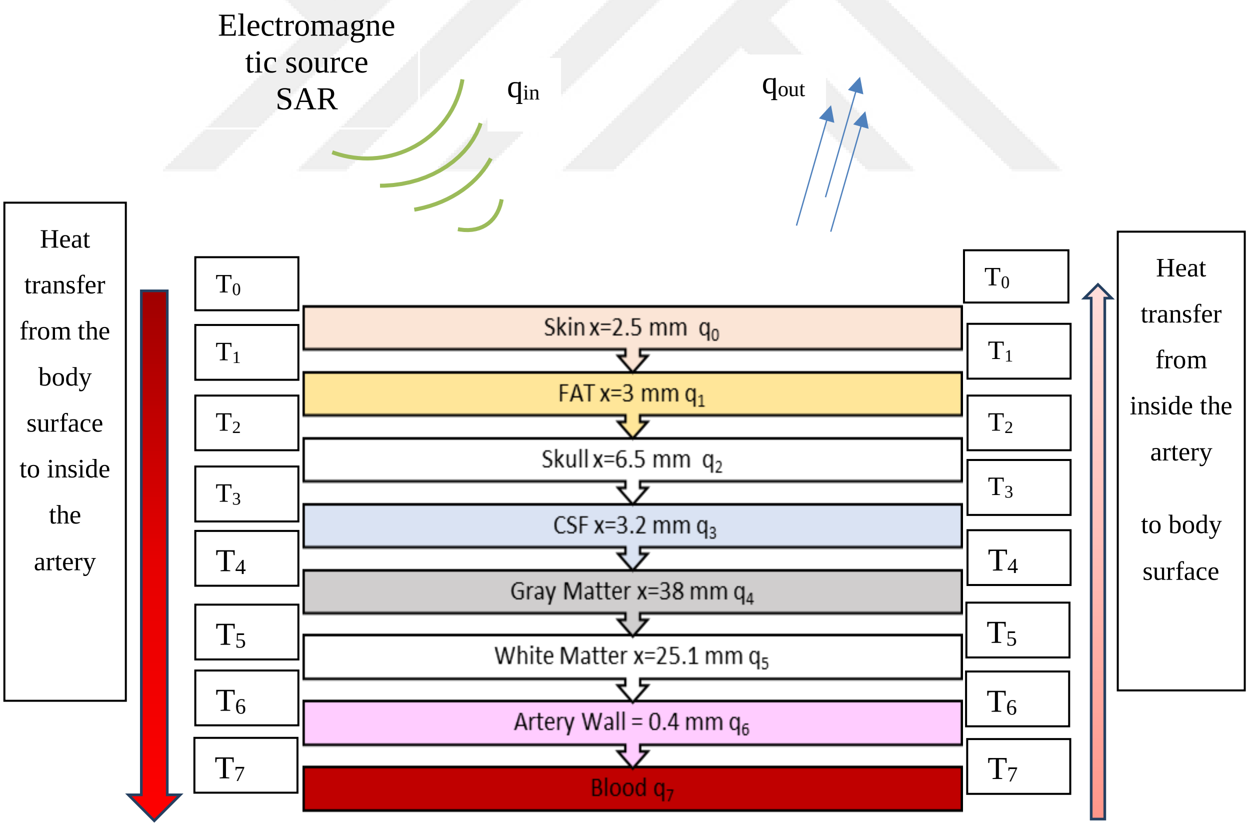

Figure 3.10: The thickness of the head's layers arranged in series with heat transfer direction.

The SAR value is based on the FCC standard is $1.6\ \frac{W}{Kg}$ [2, 40, 41, 42]. The area chosen for heat transfer through the head layers is $A = 10cm\ \times 5\ cm$.

3.3.4 Equations Required

Using the equation in [2, 13, 14, 35, 37] as the following:

According to the circuit in Fig.3. The heat transfer equation is:

$$q_{Total} = q_{Skin} = q_{Fat} = q_{Skul} = q_{CSF} = q_{Gray\ Matter} = q_{White\ Matter} = q_{Blood} \tag{3.85}$$

q is the heat transfer in watt

The equation of heat transfer conduction is

$$\mathrm{q} = -(\mathrm{KA})_{x,y,z}\,\nabla T = -(kA_x\frac{\partial T}{\partial x} + kA_y\frac{\partial T}{\partial y} + kA_z\frac{\partial T}{\partial z}) \tag{3.86}$$

x,y, and z are a coordinate system

The eqn. (3.86) represents heat transfer in three dimensions.

The mobile or the electromagnetic source in the near field is used and exerted on the human head. The direction of exposure in one dimension, the eqn. (3.86) becomes

$$\mathrm{q} = -kA_x\frac{\partial T}{\partial x} \tag{3.86}$$

k is thermal conductivity in $\frac{W}{m{\cdot}^{\circ}\mathrm{C}}$

A is the area in m^2

T is the Temperature

$\frac{\partial T}{\partial x}$ is the temperature difference in the direction of x in meter (m)

The resistance of conduction is

$$R_x = \frac{\triangle x}{kA_x} \frac{℃}{W} \tag{3.87}$$

$\triangle \boldsymbol{x}$ is layers' thickness

The heat transfer convection is

$$q = A \times h(\triangle T) = -A \times h(T_2 - T_1) \tag{3.88}$$

h is heat transfer convection coefficient or film conductance

The resistance of heat convection

$$R = \frac{1}{A_x h} \frac{℃}{W} \tag{3.89}$$

The total heat transfer can be expressed below

$$q = \frac{T_{terminate} - T_{intial}}{\sum R_i} \tag{3.90}$$

Whereas q in watt (W)

The human body considered as a close system

$$\Delta H = Q = m\, c\, \Delta T \tag{3.91}$$

Q is heat transfer in joule

H is the enthalpy

m is the layers' mass

c is the specific heat capacity

$$SAR = \frac{\Delta H}{m\Delta t} = \frac{Q}{m\Delta t} = c\frac{\Delta T}{\Delta t} \tag{3.92}$$

$$SAR = c\frac{\triangle T}{\triangle t} \cong 4186 c_H \frac{\triangle T}{\triangle t} \tag{3.93}$$

t is the time.

$$m = \rho \times A \times \triangle \boldsymbol{x} \tag{3.94}$$

ρ is the density $\frac{Kg}{m^3}$

$$\begin{aligned} m_{Total} = A \times \big(& (\rho \times \triangle \boldsymbol{x})_{Skin} + (\rho \times \triangle \boldsymbol{x})_{Fat} + (\rho \times \triangle \boldsymbol{x})_{Skull} \\ & + (\rho \times \triangle \boldsymbol{x})_{CSF} + (\rho \times \triangle \boldsymbol{x})_{Gray\ Matter} \\ & + (\rho \times \triangle \boldsymbol{x})_{White\ Matter} \big) \end{aligned} \tag{3.95}$$

$$\begin{aligned} \sum R_i = & \left(\frac{\triangle x}{KA_x}\right)_{Skin} + \left(\frac{\triangle x}{KA_x}\right)_{Fat} + \left(\frac{\triangle x}{KA_x}\right)_{Skull} + \left(\frac{\triangle x}{KA_x}\right)_{CSF} \\ & + \left(\frac{\triangle x}{KA_x}\right)_{Gray\ Matter} + \left(\frac{\triangle x}{KA_x}\right)_{White\ Matter} \end{aligned} \tag{3.96}$$

3.3.5 Equations Implementations

The equations (3.85-3.96) are used to calculate the SAR at 1.6 influence on the head's blood with initial Temperature for Blood, white Matter, and skin's surface is 37.3, 37.1, and 36.1, respectively. The time exposure is 6 minute.

The system in Fig. 3.9 (a)

Starting the equation (3.96) determine the total resistance

$\sum R_i = \frac{10^{-3}}{10^{-1} \times 5 \times 10^{-2}} \left(\left(\frac{2.5}{0.45}\right)_{Skin} + \left(\frac{3}{0.25}\right)_{Fat} + \left(\frac{6.5}{0.4}\right)_{Skull} + \left(\frac{3.2}{0.6}\right)_{CSF} + \left(\frac{38}{0.57}\right)_{Gray\ Matter} + \left(\frac{25.1}{0.5}\right)_{White\ Matter} \right)$

$R_{Total} = 31.28\ \frac{C^o}{W}$

$q = \frac{37.1 - 36.1}{31.28} = 0.03969\ W$ (3.90) It is liberated from the body (Exothermal)

$m_{Total} = 10^{-1} \times 5 \times 10^{-2} \times 10^{-3} \times \big((1010 \times 2.5)_{Skin} + (920 \times 3)_{Fat} + (1810 \times 6.5)_{Skull} + (1010 \times 3.2)_{CSF} + (1040 \times 38)_{Gray\ Matter} + (1040 \times 25.1)_{White\ Matter} \big) = 0.42953\ Kg$ (3.95)

The Heat transfer (watt per Kilogram) can be found by dividing the heat over mass

$$\left(\frac{q}{m_{total}}\right)_{liberated} = \frac{0.03969}{0.42953} = 0.0924033\ \frac{W}{Kg}$$

While the SAR can be taken1.6 $\frac{W}{Kg}$. The human body absorbs this value.

Then the Net heat transfer is absorbed by the Human body. It can be calculated as below

$$SAR_{Net} = SAR - \left(\frac{q}{m}\right)_{liberated} = 1.6 - 0.0924033 = 1.5067 \frac{W}{Kg}$$

However, Finding the Heat transfer value in watt which pass through all across the layers multiply it by mass

$q_{net} = q_{total} = SAR_{Net} \times Mass = 1.5067 \times 0.42953 = 0.64756\ W$ (Endothermal)

As consideration, the heat capacity of each layer to estimate the actual results can be utilized from equations (3.93)

$T_{int.} = 36.1$ The initial Temperature of Skin.

$$\Delta t_{second} = t_{minute} \times 60$$

$$\Delta T = \frac{SAR_{Net} \times \Delta t}{(c)_{skin}} = \frac{1.5076 \times 6 \times 60}{3500} = 0.1551\ ℃$$

$T_{New} = T_{int.} + \Delta T = 36.1 + 0.1551 = 36.251\ ℃$ The Skin's Temperature after absorbent the SAR.

Calculate the Mass of White matter from equation (3.94) as well as equation (3.85) to estimate heat transfer of white Matter ($q_{White\ Matter}$)

$$q_{Total} = q_{White\ Matter} = 0.64756$$

$$(M)_{White\ Matter} = 0.13052\ Kg$$

$$SAR_{White\ Matter} = \frac{q_{White\ Matter}}{(M)_{White\ Matter}} = \frac{0.64756}{0.13052} = 4.961385\ \frac{W}{Kg}$$

By applying (3.92)

$$\Delta T = \frac{SAR_{White\ Mattert} \times \Delta t}{(c)_{white\ matter}} = \frac{4.961385 \times 6 \times 60}{3600} = 0.49614\ ℃$$

$$(T_{White\ Mater})_{New} = (T_{White\ Mater}) + \Delta T = 37.1 + 0.49614 = 37.596\ ℃$$

Increasing the Temperature inside the White Matter.

Now, starting the calculation subsystem in Fig. 3.9 (b)

Using Dimensionless the Nusselt number to determine conduction heat coefficient. The Nusselt is 4 for vascular circulation [43-49].

$$Nu = \frac{hx}{k}$$

$$h = \frac{Nu \times k}{x} = \frac{4 \times 0.58}{8.4175 \times 10^{-3}} = 275.6\ \frac{W}{m^2 \cdot ℃}$$

$\triangle x = 0.4\ mm$ Thickness artery wall [34]

The density of artery wall $= 1300\ \frac{Kg}{m^3}$

$k_{Artery} = 0.476 \frac{W}{m^2 \cdot ℃}$

Estimate the heat transfer resistance from White Matter across the artery's wall until it reaches the blood flow center (3.87) and (3.89).

$$\sum R_i = \left(\frac{\triangle x}{KA_x}\right)_{Artery} + \left(\frac{1}{hA_x}\right)_{Blood} = \left(\frac{0.4 \times 10^{-3}}{0.476 \times 0.1 \times 0.05}\right)_{Artery} + \left(\frac{1}{275.6 \times 0.1 \times 0.05}\right)_{Blood} =$$

$$0.8938\ \frac{℃}{W}$$

Use the equation (3.90) to find the heat transfer from blood to white Matter

$q_{Blood} = \frac{37.3 - 37.1}{0.8938} = 0.223775\ W$ It represent the heat lost exothermal

The Temperature inside the center of the artery is $37.3\ ℃$

$$(q_{Blood})_{New} = q_{White\ Matter} - q_{Blood} = 0.64756 - 0.223775 = 0.42379\ W$$

The above value represents endothermal results.

3.3.6 Calculating the Total Mass of Artery and Blood

According to the Fig. 3.7 the blood flowrate $(\dot{Q})$ in the brain can be calculated as shown below

$$(\dot{Q})_{Brain} = (\dot{Q})_{heart} \times 15\% = 5 \times 15\% = 0.75 \frac{l}{min}$$

The total mass of the artery wall and the blood flow rate at 6 min can be estimated

$$(Mass)_{Total} = Artery's\ Mass + Blood's\ Mass\ in\ six\ minute = \rho \times A \times \triangle \boldsymbol{x} + \rho \times (\dot{Q})_{Brain} \times \Delta t$$

$$(Mass)_{Total} = 1300 \times 0.1 \times 0.05 \times 0.4 \times 10^{-3} + 1060 \times 0.75 \times 10^{-3} \times 6 = 4.7726\ Kg$$

$$SAR_{Blood} = \frac{(q_{Blood})_{New}}{(Mass)_{Total(Artery\ ,Blood)}} = \frac{0.42379}{4.7726} = 0.0884 \frac{W}{Kg}$$

According to equation (3.92)

$$\Delta T = \frac{SAR_{Blood} \times \Delta t}{(c)_{blood}} = \frac{0.0884 \times 6 \times 60}{3900} = 8.16 \times 10^{-3}\ ℃$$

$$T_{New\ ,Blood} = T_{Blood} + \Delta T = 37.3 + 8.16 \times 10^{-3} = 37.30816\ ℃$$

3.3.7 Aggregate Results with Different SAR Values and Time into Tables

The calculation can be inserted in the table and repeated the calculation in different SAR 4, 6, and 10 with various time exposure in minutes 6, 15, 30, 60, 120, 180, 240, 1440 2880.

Table 3.4: The results with different SAR 4, 6, and 10 with various time exposure in minutes 6, 15, 30, 60, 120, 180, 240, 1440, 2880.

SAR =1.6 W/Kg	SAR net=1.5067 W/Kg	heat transfer until white matter = 0.64756 W	heat transfer artery and blood=0.42379 W	
time in min	Total mass	SAR blood W/Kg	ΔT	Temp
6	4.7726	0.088796463	0.008196597	37.3081966
15	11.9276	0.035530199	0.008199277	37.30819928

Table 3.4: The results with different SAR 4, 6, and 10 with various time exposure in minutes 6, 15, 30, 60, 120, 180, 240, 1440, 2880. (table continued)

SAR =1.6 W/Kg	SAR net=1.5067 W/Kg	heat transfer until white matter = 0.64756 W	heat transfer artery and blood=0.42379 W	
time in min	Total mass	SAR blood W/Kg	ΔT	Temp
30	23.8526	0.017767036	0.00820017	37.30820017
60	47.7026	0.008884002	0.008200617	37.30820062
120	95.4026	0.004442122	0.008200841	37.30820084
180	143.1026	0.002961442	0.008200915	37.30820092
240	190.8026	0.002221091	0.008200953	37.30820095
1440	1144.8026	0.000370186	0.008201046	37.30820105
2880	2289.6026	0.000185093	0.008201055	37.30820106
SAR =4 W/Kg	SARnet=3.9075967 W/Kg	heat transfer until white matter = 1.678430011 W	heat transfer artery and blood=1.454655011 W	
time in min	Total mass	SAR blood W/Kg	ΔT	Temp
6	4.7726	0.304792987	0.028134737	37.32813474
15	11.9276	0.121957058	0.028143937	37.32814394
30	23.8526	0.060985176	0.028147004	37.328147
60	47.7026	0.03049425	0.028148538	37.32814854
120	95.4026	0.015247541	0.028149306	37.32814931
180	143.1026	0.010165119	0.028149561	37.32814956
240	190.8026	0.007623874	0.028149689	37.32814969
1440	1144.8026	0.00127066	0.028150009	37.32815001
2880	2289.6026	0.000635331	0.028150041	37.32815004

Table 3.4: The results with different SAR 4, 6, and 10 with various time exposure in minutes 6, 15, 30, 60, 120, 180, 240, 1440, 2880. (table continued)

SAR =6 W/Kg	SAR net=5.9075967 W/Kg	heat transfer until white matter = 2.537490011 W	heat transfer artery and blood=2.313715011 W	
time in min	Total mass	SAR blood W/Kg	ΔT	Temp
6	4.7726	0.484791311	0.044749967	37.34474997
15	11.9276	0.19397993	0.044764599	37.3447646
30	23.8526	0.097000537	0.044769479	37.34476948
60	47.7026	0.048502912	0.044771919	37.34477192
120	95.4026	0.024252117	0.044773139	37.34477314
180	143.1026	0.016168225	0.044773546	37.34477355
240	190.8026	0.012126224	0.044773749	37.34477375
1440	1144.8026	0.00202106	0.044774257	37.34477426
2880	2289.6026	0.001010531	0.044774308	37.34477431

Table 3.4: The results with different SAR 4, 6, and 10 with various time exposure in minutes 6, 15, 30, 60, 120, 180, 240, 1440, 2880. (table continued)

SAR=10 W/Kg	SAR.net=9.9075967 W/Kg	heat transfer until white Matter =4.255610011 W	heat transfer artery and blood=4.031835011 W	
time in min	Total mass	SAR blood W/Kg	ΔT	Temp
6	4.7726	0.844787958	0.077980427	37.37798043
15	11.9276	0.338025672	0.078005924	37.37800592
30	23.8526	0.169031259	0.078014427	37.37801443
60	47.7026	0.084520236	0.078018679	37.37801868
120	95.4026	0.04226127	0.078020806	37.37802081
180	143.1026	0.028174436	0.078021514	37.37802151
240	190.8026	0.021130923	0.078021869	37.37802187
1440	1144.8026	0.00352186	0.078022755	37.37802275
2880	2289.6026	0.001760932	0.078022843	37.37802284

4. DISSCUSION AND ANALYSIS

4.1 THE IMPACT OF THE FIFTH GENERATION WAVES WITH HIGH FREQUENCIES ON THE HEAD AND THEIR RESULTS WITH A NOVEL VISION

4.1.1 The SAR Penetration through the Vitro Layer (Skin)

According to the CST coordinate, the voxel model head starts at a point of approximately 12 mm of maximum SAR value in this two-dimensional graph. This point represents the power signal incident from the dipole antenna at a specific area on the head's skin. The SAR begins increasing sharply or normally until it reaches 0.281, the absorption's maximum point. The SAR evaluation keeps on penetration until drops linearly at thickness 4mm the curve continues falling exponentially till -10 mm. Therefore, the penetration takes place across 20mm through the head. On the other hand, in the same condition, when the head's power exposure value is less than the maximum SAR amount of 0.281. The SAR stays at the same distance, 12mm. This graph direction values depend on the CST coordinate and the element distribution at the CST environment.

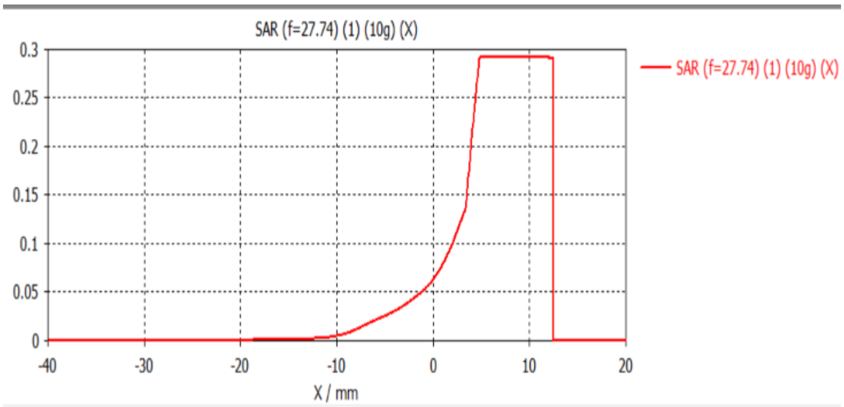

Figure 4.1: The relation between the SAR the distance (flux) layer penetration.

4.1.2 Results Analyses

The head geometry simulates the shape of the radiation pattern. The directivity has been changed (7.22 dB, 5.75 dB) when the shifting took place at the dipole location. From point (35, -40, 45) to point (35, 0, 45). The head has worked as a reflector parasitic element and changes the radiation pattern 180 degree at the head part. At a high frequency of 27.74 GHz, this paper research has found the SAR values as a function of distance, Skin depth, system sets boundary condition as well as geometrical object and angle of power incident like [50, 51].

In equation (3.3), the effect of the skin on conductivity is an enthralling phenomena. It is often used in conjunction with electrical conductors and is described as a high-frequency electric field that disperses inside a conductor. Near the surface, the current density is much higher than that of the nucleus, with an exponential decrease.

The total Energy reflection can be calculated below:

$$Eref. = Einc. - E\ abs. - E\ sust. \tag{4.1}$$

Where $E_{ref.}$ is Energy reflects from the head, $E_{inc.}$ is the incident energy on the head, $E_{abs.}$ is Energy absorbed, and $E_{sust.}$; Energy sustained on the head that present as a result of incident energy.

The sustaining power is responsible for generation reflection power when it's reached threshold values. As a result, when the high-frequency increase, the SAR decreases, the energy concentration becomes more on the surface, the absorption penetration distance decrease, and the amount of reflected energy becomes more significant according to the equation (3.3), (3.4), (3.5), (3.6) and (3.7). We can use the sustained energy and reflected energy as the harvested energy like [20].

$$E_{harvested} = E_{Ref.} + E_{Sust} \tag{4.2}$$

According to Fig. 4.1 the SAR will be Zero because the energy becomes less than the threshold value that skin starts to absorb.

The equation (4.2) helps to design the circuit for reducing the electromagnetic effects and at the same time work as harvesting energy.

Also it is possible to transfer electricity from one place to another by the body.

All energy values change when the SAR value change at the respect of antenna position.

The 5G communications almost do at high frequencies depend on the standard of that country. From this research, the outer layers, especially the parts near the surface of the human body's skin, are exposed to highly concentrated power. It is one of the reasons that cause skin cancer as the reference [16, 52]. The shield is used with a 5G mobile device to reduce the SAR effects [53, 54, 55, 56, 57, 58].

The most important thing about this study is that the SAR estimate can be found at different distances at any specific set. It becomes easy to find SAR at any point on the body and accounts for its effects.

This study becomes possible to guess the location of hazardous pathogens in part of the head layers depending on the source position of microwave sources and their operating center frequency.

In the end, the article allows us to Control the direction of the radiation reflects using the human head or all body (Beam Steering) for a 5G array antenna.

The proposed study seeks the relation the incident electromagnetic waves at high frequency on the human head for 5G mobile networks with the head response, to find several vital factors: the SAR value of the head, the penetration distance through the head layers, which head layers are effect and, The shape of radiation pattern reflection from the head, furthermore which parameters they depend as the head geometry, skin depth, conductivity of the material, source position, the distance of the source, the permittivity of the head layers. This research is very informative on the human head's behavior against microwave signals at high frequency. That enables us to know which layers of the head are most exposed to electromagnetic waves at high frequencies, helping us understand and diagnose diseases.

These results can contribute to a research leap in many medical and engineering fields, such as energy harvesting due to the high waste of energy reflected from the head and the development of fifth-generation transmitters to become more secure.

4.2 A NOVEL VISION FOR THE MATHEMATICAL MODEL BETWEEN ELECTROMAGNETIC RADIATION AND THERMODYNAMIC PARAMETERS IN BIOCHEMISTRY FRAME

This research establishes a relationship between the most critical thermodynamic factors and all electromagnetic parameters in SAR, such as (ΔH, ΔG, ΔT, ΔS, E, f, J, Q, P, δ_p and others).

When SAR is utilized properly, these characteristics play an essential function in human tissue and cell physiology by regulating the human body's reactions in order to enhance metabolism and convert nonspontaneous to spontaneous responses. Additionally, the human body is made up of many layers. We may choose which layer the electromagnetic microwave radiation penetrates, according to this study. What is the maximum depth that a microwave signal can penetrate? Additionally, which layer undergoes the reaction or decomposition in order to enhance kinetics reactions? Consider the following while attempting to fulfill these requests or dements: The frequency value defines the layer depth and type, as well as the quantity of power exposure incident on the body, which is used to calculate the SAR amount product. The holding time or exposure time necessary to complete the reaction, the skin penetration depth, and the geometrical shape of the body or exposure region. The article study demonstrates how to profit from utilizing SAR to regulate body metabolism, namely the Krebs cycle. Apart from illness treatment and physical therapy, Hair should be removed from the skin (in the cosmetic). On the other side, how dangerous uncontrolled SAR may be avoided or mitigated.

Finally, SAR principles have an exponential effect on biological reactions in the body.

4.3 THE HYPERTHERMIA CALCULATING IN HEAD BLOOD BY THE SARS INFLUENCE IN NOVEL VISION

4.3.1 Results Representations and Analysis

The results of the table can be translated into a chart as given below.

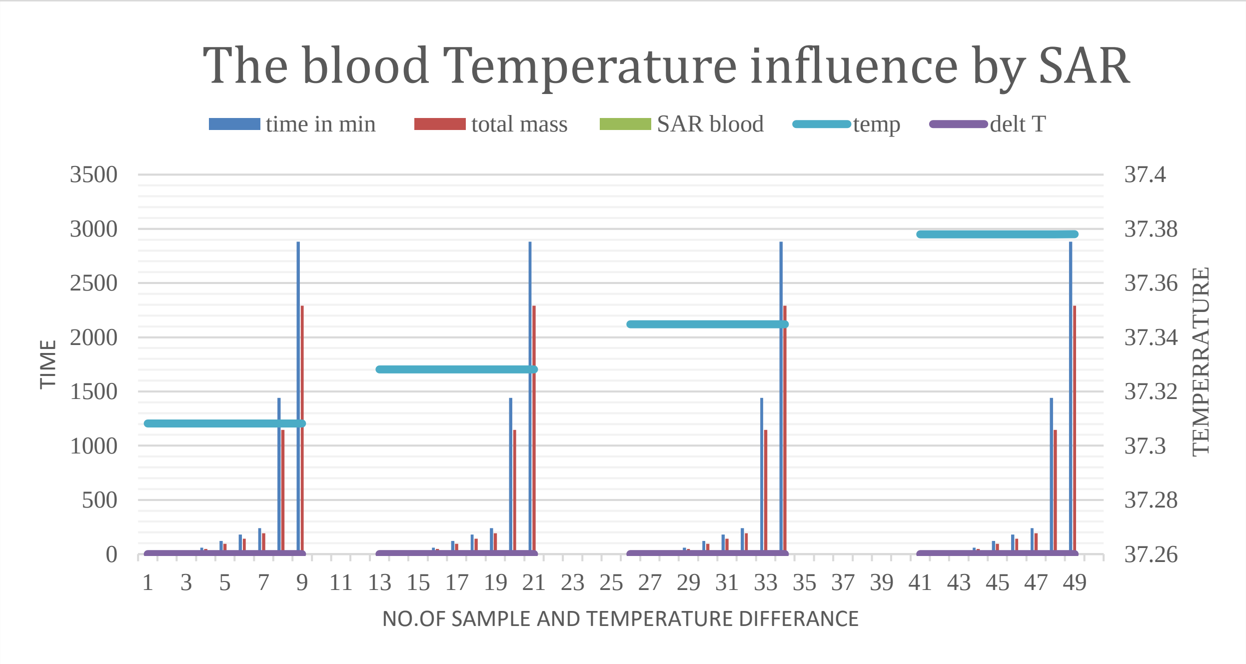

Figure 4.2: Representation of the results in the table

The Fig.4.2 shows the 4th group in deference SAR; each group contains the 9th sample with alternative exposure time from 6 minutes to a couple of days. The duration of exposure is directly proportional to the Mass of Blood. The Mass of Blood is calculated from the flow rate. As the time increased the SAR, more blood flowed through the artery that period. In this figure, the SAR value and Temperature varying are small values as comparing the time and mass. The below figure is more significant than the above figure for sensing the SAR and Temperature changing.

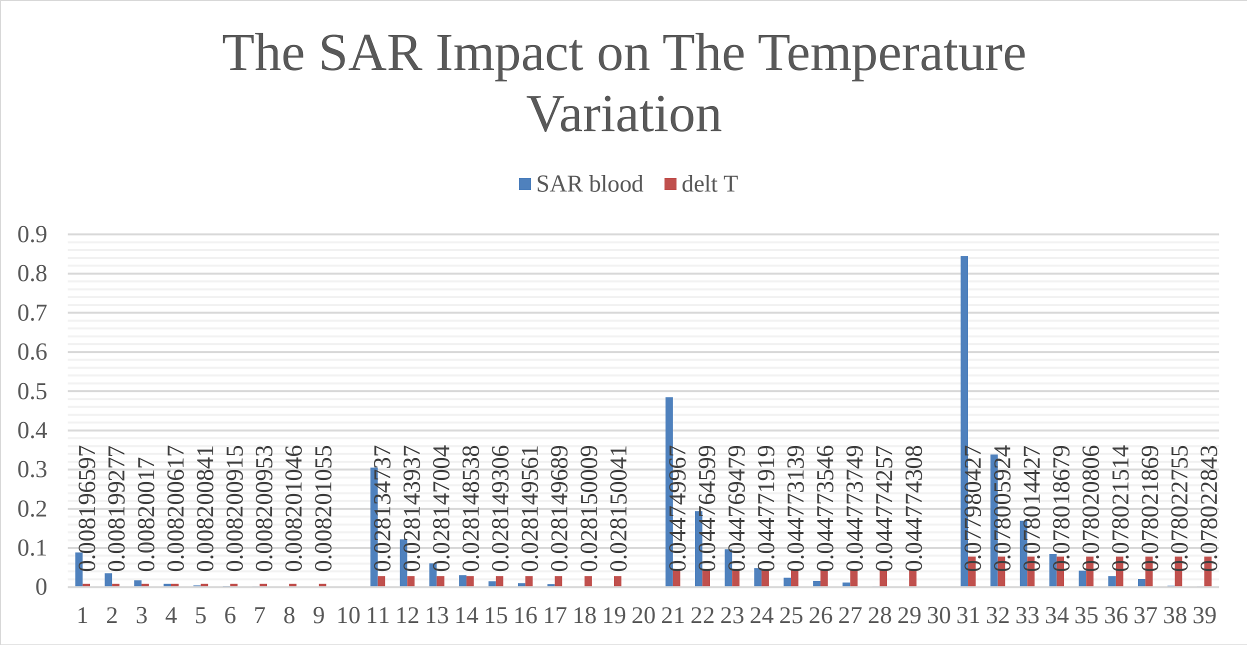

Figure 4.3: The SAR Impact on the temperature varying in the blood

In the above fig.4.3. The temperature change with time is affected by the different SAR values (1.6, 4, 6, and 10). This alternating is small from 37.3 (without SAR) to 37.37802284 (SAR=10) the total alternating of temperature is 0.07802284. As a result, the dramatic value of blood's specific heat capacity governs decreasing the changing of Blood's Temperature and the temperature differential depending on the pace and amount at which the fluid (Blood) takes heat away. Therefore, it is possible that the temperature differential in the artery wall on the blood flow in the artery.

There are two main factors to increase the Temperature in Blood: Exposure time and the SAR value. According to the chart and table, the SAR values are more significant than the time exposure's effectiveness.

This proposed study introduces SAR as a function of Mass, Temperature, specific heat capacity, and exposure time.

The dangerous case when the blood temperature reaches $(42-43)℃$ due to electromagnetic radiation to avoid this. Put some standardization on the worker site.

For further clarification, consider the following case:

All businesses are involved in the area of electromagnetic waves. During office hours, workers or employees exposure to the RF. Employers can establish blood hyperthermia guidelines for their executive workers, especially in environments where the head is exposed to these waves. It contains essential information from their employees, such as CT scans, MRIs, and Doppler devices.

For example, the company desires that SAR account make the Temperature reach 37.9 for safety, especially in workplaces with radio pollution.

We presume that the same thickness of the head layers and area exists. Besıdes takıng advantage of the results part. The time is taken 6 min.

By applying the equations presented in this research study and reversing the calculation steps. The following results are easy to find:

$$SAR = c_{blood}\frac{\Delta T}{\Delta t} = \frac{37.9 - 37.3}{6 \times 60} \times 3900 = 6.5\,\frac{W}{Kg}$$

$$q_{Bloodnew} = 6.5 \times 4.7726\,Kg = 31.0219\,W$$

$$q_{White\ Matter} = q_{Bloodnew} + q_{Blood\ exothermal\ at\ 37.3}$$

$$q_{White\ Matter} = 31.0219 + 0.223775 = 31.245675\ \mathrm{W}$$

$$q_{total} = q_{White\ Matter}$$

$$SAR_{net} = \frac{q_{total}}{m_{total\ layers}} = \frac{31.245675}{0.42953\,Kg} = 72.74387121\,\frac{W}{Kg}$$

$$SAR_{Requird} = \mathrm{SAR}_{net} + \left(\frac{q}{m_{total}}\right)_{liberated}$$

$$SAR_{Required} = 72.74387121\,\frac{W}{Kg} + 0.0924033\,\frac{W}{Kg} = 72.83627451\,\frac{W}{Kg}$$

Table 4.1: Case study calculations

SAR blood W/Kg	6.5
q_{Blood} W	31.0219
$q_{Total} = q_{White\ Matter}$	31.245675
SAR $_{net}$	72.74387121
SAR W/Kg	72.83627451

The SAR in work station must not exceed $72.83627451\ \frac{W}{Kg}$ to maintain the Temperature at $37.9\ ℃$

4.3.2 Discussion

The study has reported the effect of SAR on hyperthermia in the head's blood. The results showed that the SAR value is a substantial factor affecting the temperature rise inside the head [59, 60]. The second influencing factor is the period for exposure or absorption of radiation. The area of the layer exposed to radiation is also taken into consideration. However, these factors are restricted by factors related to the thermodynamic properties of the layer of thermal conductivity (thermal conductivity coefficient and load conduction coefficient), from heat gain and loss in addition to layer thickness, specific heat capacity, layer density. The specific heat capacity is a very influential factor in reducing temperature changes because it has considerable value for each layer of the head and each layer's mass. Especially the blood flowrate takes the heat away, as mention before.

Some pathological conditions may reduce the volumetric flow rate, such as sickle cell disease (SCD), increasing the blood temperature change [61].

The body's blood heat may lead to less temperature change since the blood in the head forms 15% of the blood of the heart pumps. The blood's heat comes from the head dilutes by 85% of the body's total blood amount.

This study touches on two important points:-

a. The specific heat capacity act as a cross-section area of wire when its increase decreases the temperature varying on the wire resistance (layer).While the conductivity depends on the material of wire and the dielectrically constant, which is one of the characteristics of the wire

b. The conductivity may be increasing by adding some additive like salts or decreasing if the rusty (fouling) (forms film in the wire’s surface) whereas in the biological tissues alters by change concentration ingredients.

Therefore in this presented study, when the human eats some salty food, it may be affected the value of conductivity. Another change occurs when increasing or decreasing the blood sugar affected on the dielectric constants causes varying in electrical properties materials. In these cases, the material has different values of dielectric constant. Use the Cole-Cole model to closing the correct result but not accuracy. Therefore the study calculation depends on the thermodynamic characteristics [62-67].

According to the above point, this paper's research is introduced precisely because it considers the mass and specific heat capacity and thermal conductivity in each layer. Another important thing the levels of calculation difficulties are more straightforward than the other method.

These calculations’ approaches are very beneficial for thermal estimation by SAR affecting head' blood easily without the complexity and high efficiency. This method applies not only to the head but also can be to apply the whole body. The research is applicable in every field relating to RF waves to account for the workers' temperature change.

This paper calculates the heat forming in the head's blood from the different SARs' influence values to consider the head's layers. The research depends on SAR's equations and heat transfer equations (Fourier's law of heat conduction and Newton's law for cooling or convection heat transfer) and thermodynamics equation. These calculations give an accurate picture of the SAR effect on the change in the head's blood temperature and the factors controlling that. This study granted a new method in the thermal calculations generated from the sources of electromagnetic waves and their absorption through the skin with high accuracy and ease of finding results. The results obtained depend on the thickness and mass of each layer and the area that the radiation penetrates with the time of exposure to the radiation. It was found the change in the temperature of the blood in the head varies slightly with time and the SAR values that were chosen. These results give a clear idea of the body's defense against radiological changes. These mathematical models can be applied to finding the temperature change in every layer as well as on all parts of the body. It is also possible to calculate the temperature that leads to a change in the vital blood characteristics. This study can be adopted in all fields that contain electromagnetic radiation. Its effect can be examined for people who work in this field periodically. The body mass index may also be included in the calculations.

5. CONCLUSIONS

The main title of the thesis is (A Novel Approach for Investigation of Electromagnetic Impact on Human Body and Its Response Analysis), which involves three leading research are submitted. Firstly the electromagnetic waves, which represent 5G Radiofrequency 27.5 GHz, influence the human head. This research gives worthy information about the wave incident. The energy of wave incident can be divided into absorption (SAR), Reflection, and sustain energy. It also gave us a clear picture of to what extent it is possible to benefit from the remaining energy and the reflected energy and to which layer of the head the electromagnetic waves reach. Secondly, the research is reported a novel vision for a mathematical model between electromagnetic radiation and thermodynamic parameters in a biochemistry frame. This research deals with the effect of electromagnetic waves on the metabolic reactions of the human body and how to link SAR equations to physical chemistry equations and express them in a biochemistry framework, which gives a new vision for the control of interactions through radio waves. This research opens new horizons for driving metabolism reactions that did not exist previously. The study contained many equations, numbering 78, explaining the connection of more than one specialty and its relationship to electromagnetic waves where a number of equations have been created that did not exist. Finally, "the hyperthermia calculating in head blood by the SARs influence in novel vision" has been studied the influence of electromagnetic energy converting to heat energy that causes the hyperthermia of the head layers. Exposure time and the SARs values in the increasing heat in head layers are two crucial factors. This study has been submitted easy new approach mathematical models to describe heat transfer throughout the head layers using Fourier's law of heat conduction and Newton's law for cooling or convection. This method can be considered more efficient and precise than the previous researches.

6. REFERENCES

[1] M. Wang *et al.*, "*Evaluation and optimization of the specific absorption rate for multiantenna systems,*" IEEE Trans. Electromagn. Compat., vol. 53, no. 3, 2011, doi: 10.1109/TEMC.2011.2109005.

[2] D. A. Sánchez-Hernández, *High frequency electromagnetic dosimetry*. Artech House, 2009.

[3] X. Zhang, "*Accurate wideband measurement of human body absorption cross section in reverberation chamber: A morphological parameters study from 1 GHz to 18 GHz,*" University of York, 2017.

[4] F. Sagnard, "*Analvtical Modeling of Insulated Dipole Applicators for Interstitial Hyperthermia: a Review,*" RADIOENGINEERING-PRAGUE-, vol. 16, no. 2, p. 20, 2007.

[5] K. Kamardin, M. K. A. Rahim, P. S. Hall, N. A. Samsuri, M. E. Jalil, and M. F. Abd Malek, "*Textile diamond dipole and artificial magnetic conductor performance under bending, wetness and specific absorption rate measurements,*" Radio Eng., vol. 24, no. 3, pp. 729–738, 2015.

[6] S. Stølen and T. Grande, *Chemical thermodynamics of materials: macroscopic and microscopic aspects*. John Wiley \& Sons, 2004.

[7] G. D. Fasman, *CRC Handbook of Biochemistry and Molecular Biology: Proteins*. CRC press, 2018.

[8] K. E. Murphy, *Thermodynamics Problem Solving in Physical Chemistry: Study Guide and Map*. CRC Press, 2020.

[9] D. A. Beard and H. Qian, *Chemical biophysics: quantitative analysis of cellular systems*, vol. 126. Cambridge University Press Cambridge, 2008.

[10] B. Biswas, A. Karmakar, and V. Chandra, "*Hilbert curve inspired miniaturized MIMO antenna for wireless capsule endoscopy,*" AEU-International J. Electron. Commun., vol. 137, p. 153819, 2021.

[11] Z. Pšenáková and M. Be\vnová, "*Evaluation of SAR (Specific Absorption Rate) in multilayer structure of biological tissues near ear with cochlear implant,*" in 2017 18th

International Conference on Computational Problems of Electrical Engineering (CPEE), 2017, pp. 1–3.

[12] K. Varshini and T. R. Rao, “*Estimation of specific absorption rate using infrared thermography for the biocompatibility of wearable wireless devices,*” Prog. Electromagn. Res. M, vol. 56, pp. 101–109, 2017.

[13] J. P. HOlman, “*Heat Transfer Ninth Edition, MCGrawHill,*” Inc., New York, USA, 2002.

[14] P. A. Rock, *Chemical thermodynamics*. University Science Books, 2013.

[15] I. Dergham, Y. Alayli, R. Imad, and Y. Hamam, “*Effects of a wireless charging system built for an electric kick scooter on human biological tissue,*” Int. J. Environ. Res. Public Health, vol. 17, no. 8, p. 2662, 2020.

[16] R. Goyal and R. Bhargava, “*FEM simulation of EM field effect on body tissues with bio-nanofluid (blood with nanoparticles) for nanoparticle mediated hyperthermia,*” Math. Biosci., vol. 300, pp. 76–86, 2018.

[17] R. Gaffoglio, M. Righero, G. Giordanengo, M. Zucchi, and G. Vecchi, “*Fast Optimization of Temperature Focusing in Hyperthermia Treatment of Sub-Superficial Tumors,*” IEEE J. Electromagn. RF Microwaves Med. Biol., 2020.

[18] T. Nagaoka et al., “*Development of realistic high-resolution whole-body voxel models of Japanese adult males and females of average height and weight, and application of models to radio-frequency electromagnetic-field dosimetry,*” Phys. Med. \& Biol., vol. 49, no. 1, p. 1, 2003.

[19] A. Nozariasbmarz et al., “*Review of wearable thermoelectric energy harvesting: From body temperature to electronic systems,*” Appl. Energy, vol. 258, p. 114069, 2020.

[20] P. Xia, R. W. Heath, and N. Gonzalez-Prelcic, “*Robust analog precoding designs for millimeter wave MIMO transceivers with frequency and time division duplexing,*” IEEE Trans. Commun., vol. 64, no. 11, pp. 4622–4634, 2016.

[21] C. A. Balanis, *Antenna theory: Analysis And Design*. John wiley \& sons, 2015.

[22] M. Tareq, D. A. Alam, M. Islam, and R. Ahmed, “*Simple half-wave dipole antenna analysis for wireless applications by CST microwave studio,*” Int. J. Comput. Appl., vol.

94, no. 7, 2014.

[23] A. C. Metaxas and R. J. and Meredith, *Industrial microwave heating*, no. 4. IET, 1983.

[24] J. Koolman, K.-H. Röhm, J. Wirth, and M. Robertson, "*Color atlas of biochemistry*," 2005.

[25] F.-Z. Tohidi et al., "*Long-term exposure to electromagnetic radiation from mobile phones can cause considerable changes in the balance of Bax/Bcl2 mRNA expression in the hippocampus of mice,*" Electromagn. Biol. Med., vol. 40, no. 1, pp. 131–137, 2021.

[26] A. Ibrahiem, C. Dale, W. Tabbara, and J. Wiart, "*Analysis of the temperature increase linked to the power induced by RF source,*" Prog. Electromagn. Res., vol. 52, pp. 23–46, 2005.

[27] B. Rubik and R. R. Brown, "*Evidence for a Connection Between COVID-19 and Exposure to Radiofrequency Radiation from Wireless Telecommunications Including Microwaves and Millimeter Waves,*" 2021.

[28] K. M. Manoj, "*Aerobic respiration: Criticism of the proton-centric explanation involving rotary adenosine triphosphate synthesis, chemiosmosis principle, proton pumps and electron transport chain,*" Biochem. insights, vol. 11, p. 1178626418818442, 2018.

[29] L. S. Costanzo, "*BRS Phisiology (Board Review Series).*" Philadelphia: Wolters Kluwer, 2018.

[30] S. Jeton, C. Selim, and B. Sadi, "*MRA study of anatomical variations of circulus arteriosus cerebri in healthy adults of Kosova,*" Egypt. J. Radiol. Nucl. Med., vol. 49, no. 4, pp. 1110–1118, 2018.

[31] Ž. N. Savić, I. I. Soldatović, M. D. Brajović, A. M. Pavlović, D. R. Mladenović, and V. D. Škodrić-Trifunović, "*Comparison between carotid artery wall thickness measured by multidetector row computed tomography angiography and intimae-media thickness measured by sonography,*" ScientificWorldJournal., vol. 11, pp. 1582–1590, 2011.

[32] K. Wendel, D. Stoliar, J. Malmivuo, and J. Hyttinen, "*Measuring tissue thicknesses of the human head using centralized and normalized trajectories,*" in Proceedings of the conference Consciousness and its Measures, 29.11.-1.12. 2009, St. Raphael hotel, Limassol, Cyprus, 2009, pp. 112–113.

[33] R. L. Boylestad, *Introductory Circuit Analysis: Pearson New International Edition: UEL*. Pearson Higher Ed, 2013.

[34] B. L. Theraja, *A textbook of electrical technology*. S. Chand Publishing, 2008.

[35] J. Jin, *Electromagnetic analysis and design in magnetic resonance imaging*. Routledge, 2018.

[36] R. S. Kshetrimayum, "*Mobile phones: Bad for your health?,*" IEEE Potentials, vol. 27, no. 2, pp. 18–20, 2008.

[37] R. R. Cano, "*Integration of mm-Wave Antenna Systems in 5G Mobile Terminals,*" 2020.

[38] J. Werner and H. Brinck, "*A three-dimensional vascular model and its application to the determination of the spatial variations in the arterial, venous and tissue temperature distribution,*" 2000.

[39] C. T. Leondes, *Biomechanical Systems: Techniques and Applications, Volume IV: Biofluid Methods in Vascular and Pulmonary Systems*, vol. 4. CRC Press, 2000.

[40] R. K. Banerjee, L. H. Back, Y. I. Cho, and C. Leondes, "*Computational fluid dynamics modeling techniques, using finite element methods to predict arterial blood flow,*" Biomechanical Systems Techniques \& Applications: Biofluid Methods in Vascular and Pulmonary Systems, vol. 4. CRC, 2001.

[41] Y. Zhang and H. Xie, "*The effect of a bifurcation structure on the heat transfer and temperature distribution of pulsatile blood flow,*" Int. J. Heat Mass Transf., vol. 118, pp. 663–670, 2018.

[42] G. S. Barozzi and A. Dumas, "*Convective heat transfer coefficients in the circulation,*" J. Biomech. Eng., vol. 113, no. 3, pp. 308–313, 1991.

[43] T.-C. Shih, H.-S. Kou, and W.-L. Lin, "*The impact of thermally significant blood vessels in perfused tumor tissue on thermal dose distributions during thermal therapies,*" Int. Commun. heat mass Transf., vol. 30, no. 7, pp. 975–985, 2003.

[44] J. Crezee and J. J. W. Lagendijk, "*Temperature uniformity during hyperthermia: the impact of large vessels,*" Phys. Med. \& Biol., vol. 37, no. 6, p. 1321, 1992.

[45] A. Hadjem, D. Lautru, C. Dale, M. F. Wong, V. F. Hanna, and J. Wiart, "*Study of specific*

absorption rate (SAR) induced in two child head models and in adult heads using mobile phones,” IEEE Trans. Microw. Theory Tech., vol. 53, no. 1, pp. 4–11, 2005.

[46] S. Bhattacharjee, M. Mitra, and S. R. B. Chaudhuri, “*Improved matching and SAR reduction with little angular instable AMC based ground plane,*” in 2016 IEEE MTT-S International Microwave and RF Conference (IMaRC), 2016, pp. 1–4.

[47] S. M. J. Mortazavi and others, “*5G Technology: Why Should We Expect a shift from RF-Induced Brain Cancers to Skin Cancers?,*” J. Biomed. Phys. \& Eng., vol. 9, no. 5, p. 505, 2019.

[48] P. K. Dutta, P. V. Y. Jayasree, and V. S. S. N. S. Baba, “*SAR reduction in the modelled human head for the mobile phone using different material shields,*” Human-centric Comput. Inf. Sci., vol. 6, no. 1, pp. 1–22, 2016.

[49] H. S. Ahmed and T. A. Elwi, “*SAR effect reduction using Reject Band Filter arrays for Wi-Fi portable devices,*” Int. J. Electron. Lett., vol. 7, no. 2, pp. 236–248, 2019.

[50] K. Han *et al.*, “*Magneto-dielectric nanocomposite for antenna miniaturization and SAR reduction,*” IEEE Antennas Wirel. Propag. Lett., vol. 15, pp. 72–75, 2015.

[51] M. Haridim, “*Use of rod reflectors for SAR reduction in human head,*” IEEE Trans. Electromagn. Compat., vol. 58, no. 1, pp. 40–46, 2015.

[52] S. Il Kwak, D.-U. Sim, J. H. Kwon, and Y. J. Yoon, “*Design of PIFA with metamaterials for body-SAR reduction in wearable applications,*” IEEE Trans. Electromagn. Compat., vol. 59, no. 1, pp. 297–300, 2016.

[53] M. Abdel-Mageed, C. Pelleti, and R. Mittra, “*Penta-band PIFA for SAR reduction for mobile and WLAN applications using R-card,*” in 2015 IEEE International Symposium on Antennas and Propagation \& USNC/URSI National Radio Science Meeting, 2015, pp. 374–375.

[54] O. P. Gandhi, Q.-X. Li, and G. Kang, “*Temperature rise for the human head for cellular telephones and for peak SARs prescribed in safety guidelines,*” IEEE Trans. Microw. Theory Tech., vol. 49, no. 9, pp. 1607–1613, 2001.

[55] J. Michałowska, A. Wac-Włodarczyk, and J. Kozieł, “*Monitoring of the Specific Absorption Rate in Terms of Electromagnetic Hazards,*” J. Ecol. Eng., vol. 21, no. 1,

2020.

[56] G. A. Barabino, M. O. Platt, and D. K. Kaul, "*Sickle cell biomechanics,*" Annu. Rev. Biomed. Eng., vol. 12, pp. 345–367, 2010.

[57] W. T. Sethi, M. A. Ashraf, S. A. Alshebeili, and K. Issa, "*Thumb positioning analysis of new elliptical-shaped microwave sensors for non-invasive glucose monitoring,*" Electron. Lett., vol. 54, no. 9, pp. 553–554, 2018.

[58] S. Suseela and P. Wahid, "*Non Invasive Monitoring of Blood Glucose Using Saliva as a Diagnostic Fluid,*" in SoutheastCon 2018, 2018, pp. 1–3.

[59] H. H. S. Javadi, R. Laversanne, and A. J. Epstein, "*Microwave conductivity and dielectric constant of tetramethyltetrathiafulvalene salts [(TMTTF) 2 X, X= SCN, ReO 4, SbF 6],*" *Phys. Rev. B*, vol. 37, no. 8, p. 4280, 1988.

[60] J. Ahmed, H. S. Ramaswamy, and V. G. S. Raghavan, "*Dielectric properties of butter in the MW frequency range as affected by salt and temperature,*" J. Food Eng., vol. 82, no. 3, pp. 351–358, 2007.

[61] H. Wen, "*Noninvasive quantitative mapping of conductivity and dielectric distributions using RF wave propagation effects in high-field MRI,*" in Medical Imaging 2003: Physics of Medical Imaging, 2003, vol. 5030, pp. 471–477.

[62] S. Castelló-Palacios, A. Vallés-Lluch, C. Garcia-Pardo, A. Fornes-Leal, and N. Cardona, "*Formulas for easy-to-prepare tailored phantoms at 2.4 GHz ISM band,*" in 2017 11th International Symposium on Medical Information and Communication Technology (ISMICT), 2017, pp. 27–31.

[63] A. P. Avolio, "*Multi-branched model of the human arterial system,*" Med. Biol. Eng. Comput., vol. 18, no. 6, 1980, doi: 10.1007/BF02441895.

[64] N. Westerhof, F. Bosman, C. J. De Vries, and A. Noordergraaf, "*Analog studies of the human systemic arterial tree,*" J. Biomech., vol. 2, no. 2, 1969, doi: 10.1016/0021-9290(69)90024-4.

[65] J. J. Wang and K. H. Parker, "*Wave propagation in a model of the arterial circulation,*" J. Biomech., vol. 37, no. 4, 2004, doi: 10.1016/j.jbiomech.2003.09.007.

[66] N. Stergiopulos, D. F. Young, and T. R. Rogge, "*Computer simulation of arterial flow with applications to arterial and aortic stenoses*," J. Biomech., vol. 25, no. 12, 1992, doi: 10.1016/0021-9290(92)90060-E.

[67] M. T. Islam, M. R. I. Faruque, and N. Misran, "*Reduction of specific absorption rate (SAR) in the human head with ferrite material and metamaterial*," Prog. Electromagn. Res. C, vol. 9, 2009, doi: 10.2528/PIERC09062303.